MATHEMATICAL MODELLING IN PHYSICS AND ENGINEERING

Wydawnictwo Wydziału Zarządzania
Politechniki Częstochowskiej

Częstochowa 2016

Scientific editors:

Andrzej Grzybowski
Stanisław Kukla

Technical editors:

Urszula Siedlecka
Izabela Zamorska

Cover design:

Tomasz Błaszczyk
Jock Cooper, www.fractal-recurrious.com

Based on the materials submitted by the authors

ISBN 978-83-65179-49-4

Wydawnictwo Wydziału Zarządzania Politechniki Częstochowskiej
42-200 Częstochowa, al. Armii Krajowej 36 B
tel. 34 325 04 80, dystrybucja 34 325 08 67
e-mail: wyd.wz@zim.pcz.pl

The conference Mathematical Modelling in Physics and Engineering – MMPE'16 is organized by Czestochowa Branch of Polish Mathematical Society jointly with the Institute of Mathematics of Czestochowa University of Technology.

Mathematical modelling is at the core of contemporary research within a wide range of fields of science and its applications. The MMPE'16 focuses on various aspects of mathematical modelling and usage of computer methods in modern problems of physics and engineering. The goal of this conference is to bring together mathematicians and researchers from physics and diverse disciplines of technical sciences. Apart from providing a forum for the presentation of new results, it creates a platform for exchange of ideas as well as for less formal discussions during the evening social events which are planned to make the conference experience more enjoyable.

This year's conference is organized for the 8th time. Every year the conference participants represent a prominent group of recognized scientists as well as young researchers and PhD students from domestic and foreign universities. This time we have invited speakers from Technical University of Košice, Slovakia, participants from Vasyl Stefanyk Precarpathian National University Ivano-Frankivsk, Ukraine as well as from a number of Polish higher education institutions: AGH University of Science and Technology, Jan Długosz University in Częstochowa, Maritime University of Szczecin, Czestochowa University of Technology, Poznan University of Technology, Medical University of Silesia, Cardinal Stefan Wyszyński University in Warsaw, University of Lodz.

Organizers

CONTENTS

MATHEMATICAL MODEL FOR SALICYLIC ACID RELEASE FROM OINTMENTS- COMPARISON OF EXPERIMENTAL DATA WITH MODEL PREDICTIONS

Marek Błasik [1]***, Renata Dyja*** [2]

[1]*Institute of Mathematics, Czestochowa University of Technology, Czestochowa, Poland*
[2]*Department of Applied Pharmacy and Drug Technology, Medical University of Silesia, Sosnowiec, Poland*
[1]*marek.blasik@im.pcz.pl,* [2] *rdyja@sum.edu.pl*

In this paper, we present a numerical and experimental results of release of salicylic acid suspended in ointment. The release of drug is possible by diffusion through a penetrant acceptor fluid in the ointment. The mathematical model describing this phenomenon was proposed by Higuchi [1] and is called moving boundary problem, because boundary of the domain where salicylic acid is undissolved is not known and determined as part of the solution. These types of problems are derived from heat transfer [2] and are often called Stefan problems in connection with the work of Joseph Stefan, who investigated the melting of the polar ice cap [3]. The diffusion of the solute through the dissolved ointment phase is described by parabolic partial differential equation:

$$\frac{\partial C(x,t)}{\partial t} = D\frac{\partial^2 C(x,t)}{\partial x^2}, \quad 0 < x < s(t), \quad t > 0, \tag{1}$$

supplemented with the boundary conditions

$$C(0,t) = C^*, \quad C(s(t),t) = C_s, \quad t > 0, \tag{2}$$

initial conditions

$$C(0,0) = C_s, \quad s(0) = 0, \tag{3}$$

and Stefan condition

$$(C_0 - C_s)\frac{dS(t)}{dt} = D\left.\frac{\partial C(x,t)}{\partial x}\right|_{x=s(t)}. \tag{4}$$

The mathematical model of release of salicylic acid suspended in ointment assumes that (i) diffusivity D of the salicylic acid in the ointment is constant; (ii) initial concentration of salicylic acid C_0 is greater than salicylic acid solubility C_s; (iii) ointment is heterogeneous and non-swellable. Models presented in [1] and [4] assume that drug release is into a perfect sink, with zero drug concentration

i.e. $C(0,t)=0$. This condition is well approximated if the release medium is exchanged sufficiently rapidly to keep sink conditions, or if the volume of the release medium is so large that drug concentration in the medium is negligible. In our approach we assume that C^* is a function of variable t depending on the amount of salicylic acid released.

Solution of mathematical model (1) - (4) presented in Fig. 1. was obtained by using numerical scheme based on finite difference method described in details in the papers [5,6].

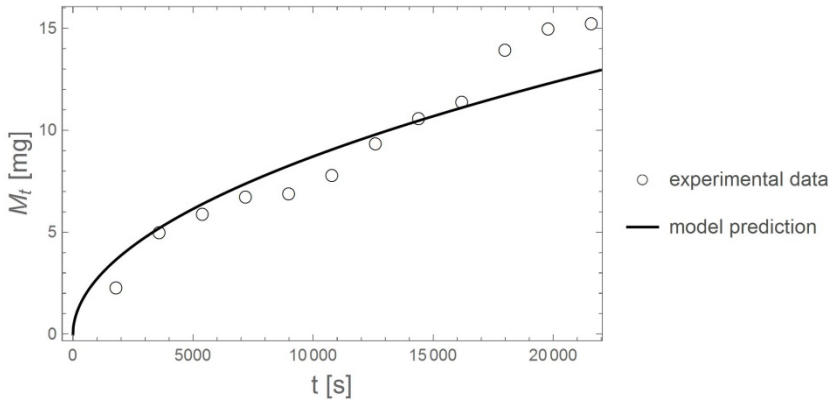

Fig. 1. Theoretical prediction (solid line) and independent experimental verification (circles) of the release of salicylic acid from eucerin ointment

Keywords: **moving boundaries problems, controlled release, partial differential equations**

References

[1] Higuchi T., Rate of release of medicaments from ointment bases containing drugs in suspension, J. Pharmac. Sci., 1961, 50, 874-875.
[2] Crank J. Free and Moving Boundary Problems, Clarendon Press, Oxford, 1984.
[3] Stefan J. Ueber einige probleme der theorie der waermeleitung. Sitzungsberichte der Ostereichischen Akademie der Wissenschaften. Mathematisch Naturwissenschaftliche Klasse 1889, 98, 473–484.
[4] Cohen, D. S., Erneux T. Free boundary problems in controlled release pharmaceuticals. II: Swelling-controlled release. SIAM J Appl Math, 1988, 48, 1466 – 1474.
[5] Schniewind J. Solution of the solidification problem of a one-dimensional medium by a new nethod. Journal of the Iron and Steel Institute, 1963, 201, 594–601.
[6] Wu Z, Luo J, Feng J. A novel algorithm for solving the classical Stefan problem. Thermal Science, 2011, 15, 39–44.

DIRECT METHODS IN FRACTIONAL VARIATIONAL CALCULUS

Tomasz Błaszczyk [1], ***Jacek Leszczyński*** [2]

[1] *Institute of Mathematics, Czestochowa University of Technology, Czestochowa, Poland*
[2] *Department of Hydrogen Energy, AGH University of Science and Technology, Krakow, Poland*
[1] *tomasz.blaszczyk@im.pcz.pl,* [2] *jale@agh.edu.pl*

The classical variational calculus is concerned with the problem of minimizing or maximizing functionals. The calculus of variations is used to create differential equations and indicate the existence of solutions. The Lagrangian and Hamiltonian formulation of dynamical systems represents one of the most important issues in physics. In this topic, functionals are dependent on derivatives of integer order.

On the other hand, one can replace (in a functional) the integer order derivative by the fractional one (for example Caputo or Riemann-Liouville derivative). Such approach leads to fractioanal variational calculus. In this case the fractional Hamiltonian and Lagrangian mechanics are described in terms of derivatives of non-integer order [1, 2]. The fractional functionals can take the following forms

$$I_L = \int_a^b L\left(x, y(x), {}^C D_{a^+}^{\alpha} y(x)\right) dx \tag{1}$$

or

$$I_R = \int_a^b L\left(x, y(x), {}^C D_{b^-}^{\alpha} y(x)\right) dx \tag{2}$$

The minimization of functionals (1) and (2) leads to the fractional differential equations which are known in literature as the fractional Euler-Lagrange differential equations. Several analytical methods to obtain solutions of these types of equations have been proposed [1, 2, 3]. However, for most fractional differential equations (especially for Euler-Lagrange equations) we cannot provide methods to determine the exact solutions. Therefore it is necessary to use numerical methods (direct or indirect).

In this work we analyse only the direct methods. We consider the following methods:

(i) The Ritz method with basis functions in the form of the modified Jacobi polynomials [4]

$$y(x) \approx y_N(x) = y_a + (y_b - y_a)\left(\frac{x}{b-a}\right)^{\alpha} + \sum_{i=1}^{N} c_i \left[x^{\alpha} \left(P_i^{(0,\alpha)}\left(\frac{2x}{b-a} - 1\right) - P_i^{(0,\alpha)}(1) \right) \right] \tag{3}$$

where $P_i^{(\alpha,\beta)}(x)$ represent the Jacobi polynomials.

(ii) The Ritz method with basis functions in the following form [5]

$$y(x) \approx y_N(x) = \sum_{i=0}^{N} c_i x^i \tag{4}$$

We compare various types of errors generated by the presented methods

$$err_1 = \int_a^b \left(y(x) - y_N(x) \right)^2 dx \tag{5}$$

$$err_2 = \max_{x \in [a,b]} \left(\left| y(x) - y_N(x) \right| \right) \tag{6}$$

$$err_3 = \max_{x \in [a,b]} \left(\left| \frac{y(x) - y_N(x)}{y(x)} \right| \right) \tag{7}$$

and estimate the rates of convergence of these methods.

Keywords: **fractional variational calculus, direct methods, fractional derivatives**

References

[1] Baleanu D., Diethelm K., Scalas E., Trujillo J.J., Fractional Calculus Models and Numerical Methods, World Scientific, Singapore, 2012.

[2] Klimek M., On Solutions of Linear Fractional Differential Equations of a Variational Type, The Publishing Office of the Czestochowa University of Technology, Czestochowa, 2009.

[3] Malinowska A.B., Torres D.F.M., Introduction to the Fractional Calculus of Variations, Imperial College Press, London, 2012.

[4] Dehghan, M., Hamedi, E.A., Khosravian-Arab, H., A numerical scheme for the solution of a class of fractional variational and optimal control problems using the modified Jacobi polynomials, Journal of Vibration and Control 2016, 22(6), 1547-1559.

[5] Jahanshahi S., Torres D.F.M., A simple accurate method for solving fractional variational and optimal control problems, Journal of Optimization Theory and Applications 2016, http://dx.doi.org//10.1007/s10957-016-0884-3.

PARALLEL IMPLEMENTATION OF FACIAL RECOGNITION SYSTEM BASED ON 2DHMM

Janusz Bobulski

Institute of Computer and Information Science,
Czestochowa University of Technology,
Czestochowa, Poland
januszb@icis.pcz.pl.pl

The constantly growing amount of digital data more and more often requires applying increasingly efficient systems for processing them. Increase the performance of individual processors has reached its upper limit, therefore, the we need to build multiprocessor systems. To exploit the potential of such systems, it is necessary to use parallel computing, i.e. creating computer systems based on parallel programming. In practice, most often their used adjusts the parallelization of the data processes, or regulates the parallelization of the query tasks. The system of face recognition that require high computational power is one of potential application of the computations parallelization, especially for large database sizes.

The aim of the research was to develop a parallel system of face recognition based on two-dimensional hidden Markov models (2DHMM). The procedure of the person' identification used for feature extraction wavelet transform in this system. The feature vector obtained from this transformation is utilized for training and testing the system. In this method, for identification purposes, both 2D and 3D images of the face were exploited. The detailed description of this sequential method of the face recognition one may find in the article [2]. Because of long computation times in this method we decided to apply the parallel processing. The analysis of algorithms of the systems using 2DHMM allowed use the parallel processing. The study of learning mode of the system allowed for the application the parallelization of data processing and the parallelization of tasks. While in test mode it was possible to uses only the parallelization of tasks. Whereas the parallelization of data processing implemented through the separation of data on the processors. One task was the processing (training or testing) of one face image. For research we used the face base UMB-DB [3]. The experiment carried on the processor Intel i5 3.3 GHz with 4 cores and 4 threads, and the results of the experiment are presented in table 1.

The results show that compared to sequential calculations, the best results were obtained for parallelization of tasks. In the learning mode and the testing mode with the use of a 2D image, we got a low acceleration of calculations, because the source data was much less. However for 3D images, a 3.2 acceleration was get for the learning mode, and 2.7 for the testing mode. In case of using for the identification both of image, 2D as well as 3D, acceleration for training mode and test was respectively 3.3 and 2.8.

Table 1. Comparison of processing time

Type of processing	Type of face image	Time of learning [s]	Time of testing [s]
Sequential	2D	126	117
Sequential	3D	1145	1090
Sequential	2D+3D	1262	1282
Parallel processing	2D	102	1632
Parallel processing	3D	762	2117
Parallel processing	2D+3D	1082	3776
Parallel task	2D	122	98
Parallel task	3D	359	401
Parallel task	2D+3D	386	451

The use of parallel data processing using *parfor* loop did not give a significant speed up calculations. This is due to the structure of training and testing algorithms of HMM, that they have in their structure the operations, that do not allow parallelization of the calculation process.

In conclusion, when we are creating a biometric system, using a face image of individuals and it is based on 2DHMM, it is worth to use parallel processing with application parallelization of tasks. In such a system, each processor independently processes one object, i.e. one person. The result of applying a parallel structure system is a three-fold reduction in computation time.

Keywords: **parallelization, face recognition, 2D hidden Markov models, HMM, parallel task**

References

[1] Culler D.E., Singh J.P., Gupta A., Parallel Computer Architecture – A Hardware/Software Approach, Morgan Kaufmann Publishers, 1999.
[2] Bobulski J., 2DHMM-Based Face Recognition Method, Image Processing And Communications Challenges 7, Advances in Intelligent Systems and Computing 2016, 389, 11-18.
[3] Colombo A., Cusano C., Schettini R., Umb-db: A database of partially occluded 3d faces, Proc. ICCV 2011 Workshops 1 (2011) 2113-2119.

APPLICATION OF DIFFERENCE EQUATIONS TO EIGENVALUES OF CERTAIN BAND MATRICES

Jolanta Borowska, Lena Łacińska

Institute of Mathematics, Czestochowa University of Technology, Czestochowa, Poland
jolanta.borowska@im.pcz.pl, lena.lacinska@im.pcz.pl

The subject of considerations are tridiagonal and 2-tridiagonal Toeplitz matrices, which are the special case of band matrices. We are show the explicit formulas for eigenvalues of the matrices under considerations.

The tridiagonal Toeplitz matrix will be denoted by $\mathbf{A}_n$, whilst the 2-tridiagonal Toeplitz matrix by $\mathbf{A}_n^{(2)}$. So, the analyzed matrices have the forms

$$\mathbf{A}_n = \begin{bmatrix} a & c & & & & & \\ b & a & c & & & & \\ & b & a & c & & & \\ & & \ddots & \ddots & \ddots & & \\ & & & \ddots & \ddots & \ddots & \\ & & & & b & a & c \\ & & & & & b & a \end{bmatrix}_{n\times n} \tag{1}$$

and

$$\mathbf{A}_n^{(2)} = \begin{bmatrix} a & 0 & c & & & & \\ 0 & a & 0 & c & & & \\ b & 0 & a & 0 & c & & \\ & \ddots & \ddots & \ddots & \ddots & \ddots & \\ & & \ddots & \ddots & \ddots & \ddots & c \\ & & & b & 0 & a & 0 \\ & & & & b & 0 & a \end{bmatrix}_{n\times n} \tag{2}$$

Let λ be an eigenvalue and $\mathbf{v} = [v_1, ..., v_n]^{\mathrm{T}} \neq 0$ be the corresponding eigenvector. Hence the eigenvalue problem for matrix (1) has the form

$$\mathbf{A}_n \mathbf{v} = \lambda \mathbf{v} \tag{3}$$

From the above equation we have

$$\left(\mathbf{A}_n - \lambda \mathbf{I}_n\right)\mathbf{v} = \mathbf{0} \tag{4}$$

where $\mathbf{I}_n$ is identity matrix of an order n and $\mathbf{0}$ is column matrix filled by zero. Eigenvector $\mathbf{v}$ is assumed to be nonzero, then λ is an eigenvalue of matrix $\mathbf{A}_n$ if and only if

$$\det(\mathbf{A}_n - \lambda \mathbf{I}_n) = 0 \tag{5}$$

It can be observed that matrix $\mathbf{A}_n - \lambda \mathbf{I}_n$ has tridiagonal Toeplitz structure. Let us denote the determinant of matrix $\mathbf{A}_n - \lambda \mathbf{I}_n$ by W_n. Following [1], we can write the recurrence equation for W_n

$$W_{n+2} - (a - \lambda)W_{n+1} + bcW_n = 0, \quad n \geq 1 \tag{6}$$

with the initial conditions of the form

$$W_1 = a - \lambda, \qquad W_2 = (a - \lambda)^2 - bc \tag{7}$$

Solution to equation (6) with initial conditions (7) depend on $\Delta = (a - \lambda)^2 - 4bc$. Assuming $\Delta \neq 0$ and bearing in mind [1], we have

$$W_n = \frac{1}{\sqrt{\Delta}}\left(p^{n+1} - q^{n+1}\right) \tag{8}$$

where

$$\begin{aligned} p &= \frac{a - \lambda + \sqrt{(a - \lambda)^2 - 4bc}}{2} \\ q &= \frac{a - \lambda - \sqrt{(a - \lambda)^2 - 4bc}}{2} \end{aligned} \tag{9}$$

Hence from (5) we have

$$p^{n+1} - q^{n+1} = 0 \tag{10}$$

After many transformations, [2], we conclude that in this case eigenvalues λ_s, $s = 1, \ldots, n$ of matrix $\mathbf{A}_n$ have the form

$$\lambda_s = a - 2\sqrt{bc}\cos\frac{s\pi}{n+1}, \; s = 1, \ldots, n \tag{11}$$

Now, let us assume that $\Delta = 0$. Hence, c.f. [1]

$$W_n = \frac{2bc + n\left((a-\lambda)^2 - 2bc\right)}{2}\left(\frac{a-\lambda}{2}\right)^{n-2} \tag{12}$$

It can be proved, [2] that in this case condition (5) leads to the following formula on eigenvalues

$$\lambda_s = a, \quad s = 1, \ldots, n \tag{13}$$

Let us observe relation (13) can be obtained from (11) under assumption $b = 0$ or $c = 0$. It means that all eigenvalues of tridiagonal matrix $\mathbf{A}_n$ can be expressed by the formula (11).

The subsequent considerations will be concerned with the eigenvalues of 2-tridiagonal matrix of the form (2). Bearing in mind the above considerations, we conclude that λ is an eigenvalue of matrix (2) if and only if

$$\det(A_n^{(2)} - \lambda I_n) = 0 \tag{14}$$

Let us denote the determinant on the left hand side of equation (14) by $W_n^{(2)}$. The derivation of the formula on eigenvalues of matrix (2) is based on the relation between determinant $W_n^{(2)}$ and determinants of pertinent tridiagonal matrices. Taking into account [3] we have

$$W_n^{(2)} = \begin{cases} \left(W_{\frac{n}{2}}\right)^2, & n \text{ is even} \\ W_{\frac{n-1}{2}} W_{\frac{n+1}{2}}, & n \text{ is odd} \end{cases} \tag{15}$$

where $W_{\frac{n}{2}}$, $W_{\frac{n-1}{2}}$, $W_{\frac{n+1}{2}}$ are the determinants of tridiagonal matrices of the form analogical as matrix (1) of orders $\frac{n}{2}$, $\frac{n-1}{2}$ and $\frac{n+1}{2}$, respectively.

It can be proved [2] that if matrix (2) has the even order *n* then its eigenvalues have the form

$$\lambda_s = a - 2\sqrt{bc}\cos\frac{2s\pi}{n+2}, \; s = 1, \ldots, \frac{n}{2} \tag{16}$$

On the other hand, when the matrix (2) has the odd order *n* then its eigenvalues can be represented by the formulas, c.f. [2]

$$\lambda_s = a - 2\sqrt{bc}\cos\frac{2s\pi}{n+1},\ s = 1,\ldots,\frac{n-1}{2} \tag{17}$$

and

$$\lambda_s = a - 2\sqrt{bc}\cos\frac{2s\pi}{n+3},\ s = 1,\ldots,\frac{n+1}{2} \tag{18}$$

The above two formulas represent n different eigenvalues of 2-tridiagonal matrix (2) of the odd order n.

Keywords: **band matrices, eigenvalues, tridiagonal matrix, Toeplitz matrix**

References

[1] Borowska J., Łacińska L, Rychlewska J., Application of difference equation to certain tridiagonal matrices, Scientific Research of the Institute of Mathematics and Computer Science 2012, 3(11), 15-20.

[2] Borowska J., Łacińska L, Eigenvalues of 2-tridiagonal Toeplitz matrix, Journal of Applied Mathematics and Computational Mechanics 2015, 14(4), 11-17.

[3] Borowska J., Łacińska L, Rychlewska J., On determinant of certain pentadiagonal matrix, Journal of Applied Mathematics and Computational Mechanics 2013, 12(3), 21-26.

MATHEMATICAL MODELING OF REMOVAL OF COLON POLYP DURING ELECTROSURGICAL POLYPECTOMY

Mariusz Ciesielski [1], Jaroslaw Siedlecki [2]

[1]Institute of Computer and Information Sciences, Czestochowa University of Technology, Czestochowa, Poland
[2]Institute of Mathematics, Czestochowa University of Technology, Czestochowa, Poland
[1]mariusz.ciesielski@icis.pcz.pl, [2]jaroslaw.siedlecki@im.pcz.pl

Colon polypectomy is used to remove abnormal growths, called polyps, from the colon (the large intestine) in order to reduce the risk of the colon cancer development [1]. Polyps can be removed endoscopically (colonoscopy). One of the popular methods of examination is the electrosurgical polypectomy. In this procedure a polypectomy snare is passed over the polyp and tightened around the stalk of the polyp. Electric current is then passed for a short period of time (a few seconds) through the snare loop to cut off the polyp stalk from the colon wall while providing electrocautery at the same time in order to close the wound and stop bleeding.

The considered polyp-colon domain (treated as the axially symmetrical object) is shown in Figure 1. The domain consists of the following subdomains: the colon tissue (Ω_1), the polyp-tissue (Ω_2) and the wire loop snare electrode (Ω_3).

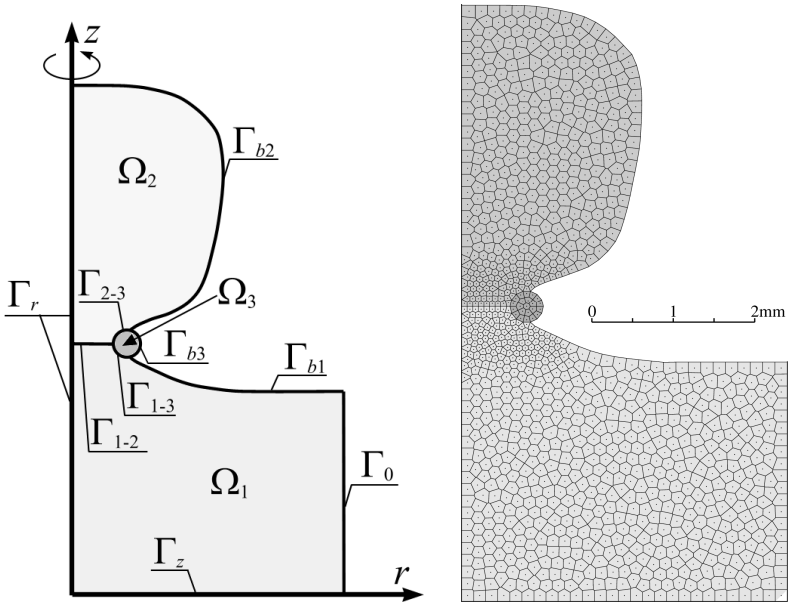

Fig. 1. The considered domain (longitudinal section) and the control volume mesh

The heating process of the colon and polyp tissues is described by the system of partial differential equations (energy equations called the Pennes equation with the Joule heating source term caused by an electric field [2]) with the adequate boundary-initial conditions. Based on the calculated temperature at a particular location in the tissue, the degree of the tissue damage can be predicted using the Henriques' damage integral (if its value belongs to the interval $(1, 10^4)$ then we deal with the 2nd degree burn; values greater than 10^4 corresponds to the 3th degree burn).

Equations of the mathematical model were solved by using the Control Volume Method [3, 4] for the mesh presented in Fig. 1. In Fig. 2 the sample results are shown. The tissue damage depends strongly on the electrical pulse duration.

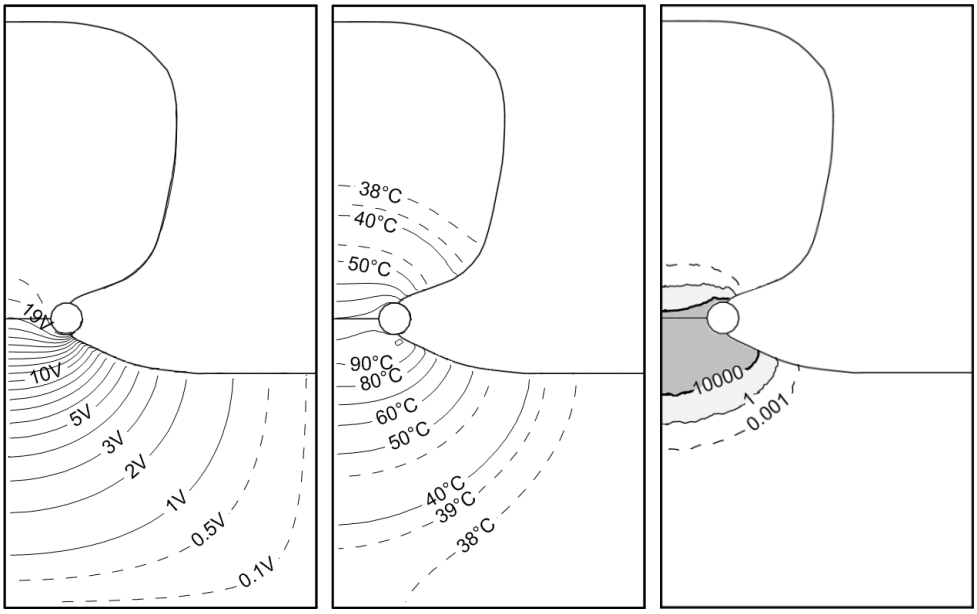

Fig. 2. Distributions of the electrical potential field, the isotherms and the predicted values of the damage integral in the considered domain for time 3 s

Keywords: **mathematical bioheat transfer modelling, biological tissue heating, polypectomy, cancer, electromagnetic field**

References

[1] Messmann H., Atlas of Colonoscopy: Examination Techniques and Diagnosis, Thieme, 2005.
[2] Majchrzak E., Dziatkiewicz G., Paruch M., The modelling of heating a tissue subjected to external electromagnetic field, Acta of Bioengineering and Biomechanics 2008, 10(2), 29-37.
[3] Siedlecki J., Ciesielski M., Simulations of thermal processes in a restored tooth, Journal of Applied Mathematics and Computational Mechanics 2013, 12 (4), 103-108.
[4] Ciesielski M., Mochnacki B., Application of the control volume method using the Voronoi polygons for numerical modeling of bio-heat transfer processes, Journal of Theoretical and Applied Mechanics 2014 52(4), 927-935.

HIERARCHICAL LOAD TRANSFER IN THE FIBRE BUNDLE MODEL OF NANOPILLAR ARRAYS

Tomasz Derda

Institute of Mathematics, Czestochowa University of Technology,
Czestochowa, Poland
tomasz.derda@im.pcz.pl

The phenomena of fracture and failure of materials are ubiquitous but mostly undesirable. Under external load materials undergo a damage process that leads to complete failure if load increase is not stopped. In this work we study breakdown processes in axially loaded metallic nanopillar arrays. To analyse failure in such systems we adapt Fibre Bundle Model which is a fundamental statistical model for failure of heterogeneous materials [1-2].

The system under consideration consists of N longitudinal nanopillars. Each nanopillar is characterised by its own strength-threshold σ_{th}^{i}, $i = 1,2,..,N$ to an applied axial load. Pillar-strength-thresholds are quenched random variables drawn according to nanoscale Weibull statistics[3]:

$$P(\sigma_{th}) = 1 - \exp\left\{ - n^{*} \left(\frac{\sigma_{th}}{\sigma_{o}} \right)^{\rho} \right\} \tag{1}$$

where n^{*} is the number of critical defects, σ_{o} and ρ are two constants. By applying nanoscale Weibull statistics simply considering $n^{*} = 1$, we assume nearly defect-free structures.

Loading of the system is realised by two different but equivalent procedures, namely quasi-static and application of finite force. When the load carried by a pillar exceeds its strength-threshold the pillar crashes and its load is transferred to other intact pillars according to a given load sharing protocol. We assume clustering of the pillars in the sense of their close arrangement. This means that effective range of interaction is restricted to pillars belonging to the same group. For this reason load transfer rule is based on hierarchical load sharing protocol [4-5]. At the lowest hierarchy level pillars form groups containing z nearest neighbours. In the second level a group of the z nearest groups from the lowest level is the neighbourhood of the order 2 *etc*. The load from the broken pillar is equally transferred to all intact pillars belonging to its neighbourhood of the lowest possible level. In our calculations number of hierarchy levels M varies from 2 to 6. z is called a coordination number.

One of the quantities most intensively studied in this work is the probability of breakdown of the system. Figure 1 shows probabilities of breakdown for six

different coordination numbers z. As can be seen breakdown probability as a function of initial load per pillar σ can be nicely fitted (dashed lines in Figure 1) by the function:

$$P(\sigma) = \frac{1}{2}\operatorname{erfc}\left(\frac{\xi - \sigma}{\sqrt{2}\omega}\right) \tag{2}$$

where ξ and ω are coefficients obtained from simulation results. Another interesting property analysed in the work is strength of the set, i.e, the mean value of load at which nanopillar array fails. We have also investigated sizes of critical avalanches and avalanche distributions.

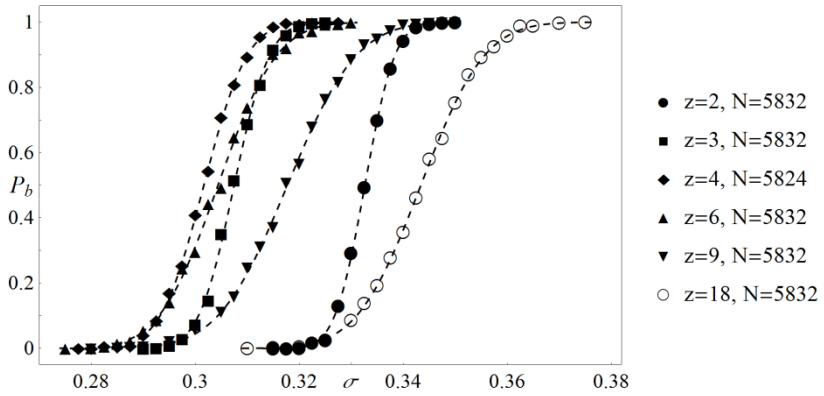

Fig.1 Empirical breakdown probability P_b as a function of initial load per pillar σ for different coordination numbers and $M = 4$. The dashed lines represent function (2) with parameters computed from simulations.

Keywords: **nanoscale, stress transfer, damage mechanics, probability and statistics, strength**

References

[1] Pradhan S., Hansen A., Chakrabarti B.K., Failure Processes in Elastic Fiber Bundles, Rev. Mod. Phys. 2010, 82, 499-555.
[2] Hansen A., Hemmer P. C., Pradhan S., The Fiber Bundle Model: Modeling Failure in Materials, Wiley 2015.
[3] Pugno N. M., Ruoff R.S., Nanoscale Weibull statistics, J. Appl. Phys., 2006, 99, 024301-4.
[4] Newman W. I., Gabrielov A. M., Failure of hierarchical distributions of fibre bundles. I, Int. J. Fract. 1991, 50(1), 1-14.
[5] Mishnaevsky Jr. L., Hierarchical Composites: Analysis of damage evolution based on fibre bundle model, Compos. Sci. Technol. 2011,71, 450-460.

AUTOMATIC CODE GENERATION FOR FINITE ELEMENT SHAPE FUNCTIONS

Andrzej Grosser, Grzegorz Michalski

Institute of Computer and Information Sciences, Czestochowa University of Technology, Czestochowa, Poland
andrzej.grosser@icis.pcz.pl, grzegorz.michalski@icis.pcz.pl

The finite elements define shape functions. Shape functions interpolates the solution between the nodal values at the mesh. Usually, these are linear functions or polynomials of low degree. Some problems, however, required the use of more complex functions, for example curvilinear, Hermitian [1].

Finite element method libraries provide the basic shape function. In most cases also they allow to add own custom, adapted to the problem functions. Unfortunately, this is not always a simple task, is required to implement a number of methods, for example that return a value of the derivative of shape function at a certain point. An additional disadvantage is the wide range of different solutions, the most hand created source code cannot be easily transferred between different libraries.

Above mentioned problems can be resolved by creating a domain specification language. Domain specification languages are small languages tailored to a particular problem domain [2]. This way can be reduced the number of details. In the case of the shape functions the domain specification language provide their general description. On the basis of this description generators automatically create the code. It is also possible to create generators that create code for the different libraries.

The article presents a simple external specification language. This language allows to generate the source code for the library TalyFEM [3]. It is a library of Finite Element Method and allows creation of scalable software engineering. It provides only the triangular and tetrahedral elements linear shape functions.

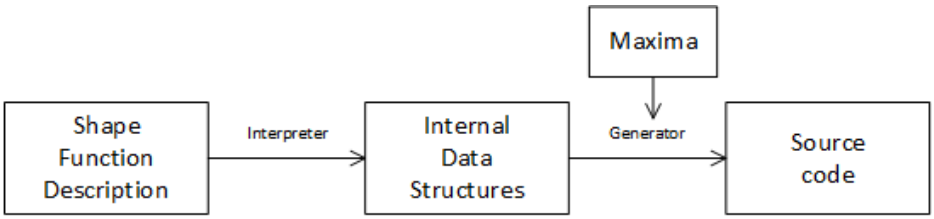

Fig. 1. Source code generation from shape function description

Figure 1 shows the process of generating the source code based on the supplied shape function. The interpreter reads the specification shape functions and creates internal data structures independent of the concrete syntax of domain specific

language. Then, on the basis of these data generator, with the help of a mathematical program Maxima (for example to determine the derivative of the shape function), is able to create the target source code.

Keywords: **finite element method, shape functions, automatic code generation**

References

[1] Zienkiewicz O. C, Taylor R. L. The Finite Element Method: The basis, Butterworth-Heinemann, 2000
[2] van Deursen A., Klint P., Visser J. Domain-Specific Languages: An Annotated Bibliography ACM SIGPLAN Notices 2000, 35(6), 26-36
[3] Kodali H.K., Ganapathysubramanian B., A computational framework to investigate charge transport in heterogeneous organic photovoltanic devices, Computer Methods in Applied Mechanics and Engineering 2012, 247, 113–129

THE USE OF MULTICORE ARCHITECTURES FOR NUMERICAL CALCULATION OF DENDRITIC SOLIDIFICATION

Kamil Halbiniak, Adam Kulawik

Institute of Computer and Information Sciences, Czestochowa University of Technology, Czestochowa, Poland
kamil.halbiniak@icis.pcz.pl adam.kulawik@icis.pcz.pl

Presented numerical model developed by Warren and Bottingera is used to determine the size of the solidified area in case of growth of dendritic grain. In this model, the growth of microstructure is determined by the solution of the phase content equation:

$$\frac{1}{M_\phi}\frac{\partial \phi}{\partial t} = \varepsilon^2\left[\nabla\cdot(\eta^2\nabla\phi) + \eta\eta'\left(sin(2\theta)\left(\frac{\partial^2\phi}{\partial y^2}-\frac{\partial^2\phi}{\partial x^2}\right)+2cos(2\theta)\frac{\partial^2\phi}{\partial x\,\partial y}\right)\right]$$
$$-\frac{1}{2}(\eta'^2+\eta\eta'')\left(-cos(2\theta)\left(\frac{\partial^2\phi}{\partial y^2}-\frac{\partial^2\phi}{\partial x^2}\right)+2sin(2\theta)\frac{\partial^2\phi}{\partial x\,\partial y}-\frac{\partial^2\phi}{\partial x^2}-\frac{\partial^2\phi}{\partial y^2}\right) \quad (1)$$
$$-cH_B-(1-c)H_A-cor$$

and the equation defining the concentration of alloy [1,2,3]. In the equation above $M\varphi$ is defined as the solid/liquid interface mobility, ε is a parameter related to the interface width, η is the anisotropy factor, H_A and H_B denotes the free energy of both components, *cor* is the stochastic factor which models thermodynamic fluctuations near the dendrite tip. The concentration of alloy is determined based on the solution of the diffusion equation defined as:

$$\frac{\partial c}{\partial t} = \nabla\cdot D_c[\nabla c + \frac{V_m}{R}c(1-c)(H_B(\phi,T)-H_A(\phi,T))\nabla\phi] \quad (2)$$

where: D_c is the diffusion coefficient, V_m is the specific volume, R is the gas constant. Due to the occurring derivatives of the second order and the mixed derivatives to determining these values the generalized finite difference method is used.

Modern heterogeneous computing platforms have become powerful HPC solutions, which could be applied for a wide range of applications [4,5]. An example of this trend are hybrid platforms containing Intel Xeon Phi coprocessors. These solutions offer similar performance advantages to traditional platforms based on CPUs only. It should be noted that the main advantages of heterogeneous Intel CPU-MIC platforms is capability of running applications written in industry standard programming languages [6]. However, there is still an open issue how scientific applications can utilize efficiently the hybrid platforms containing Intel Xeon Phi coprocessors [7,8].

In our previous work, we developed an approach for porting and optimizing a real-life scientific application for modelling alloy solidification on computing platforms with a single Intel Xeon Phi accelerator [7]. This paper outlines a method of porting and optimization solidification application to hybrid platforms equipped with Intel Xeon Phi coprocessors. The main computational core of studied application is responsible for parallel calculation for subsequent of time steps and writing partial results after the first and then after every 2000 time steps. The original version of application utilize two CPUs only and in this version computations are interleaved with data writing. Proposed approach allows us to take advantage of all resources of hybrid platforms containing two coprocessors and two CPUs. This paper present also a sequence of steps that are necessary for porting studied application to platforms with accelerators, assuming no significant modifications of the code. The main challenges associated with proposed approach include overlapping of data movements and writing partial results to the file with computation carried out by the CPU, but also utilize core/threads and vector processing units offered by the processors as well as the coprocessors. To employ all available resources of utilized platforms we use heterogenous programming model which is a combination of OpenMP parallel programming standard and offload programming model for Intel MIC architecture. Idea of adaptation studied application to hybrid platform with Intel MIC is shown in Figure 1.

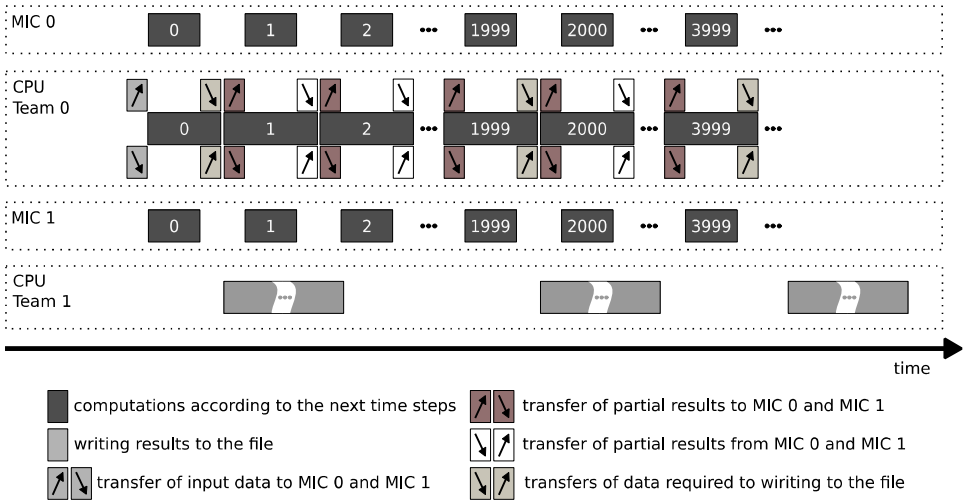

Figure 1. Idea of adaptation numerical model of solidification to hybrid CPU-MIC platforms

In this study, we use two hybrid platforms equipped with CPUs and Intel Xeon Phi coprocessors [9]. The first platform contains two Haswell-EP based Intel Xeon E5-2699 v3 CPUs, 256GB of DDR4-2133 main memory and two top-of-the-line Intel Xeon Phi 7120P coprocessors. Each of CPUs includes 18 cores clocked at 2.3 GHz, while single coprocessor contains 61 cores clocked at 1.238 GHz with 16 GB main memory. The second platform combines two Intel Xeon E5-2695 v2 CPUs

(Ivy Bridge-EP architecture), 128 GB of DDR3-1866 main memory and two Intel Xeon 7120P coprocessors. Each of processors contains 12 cores clocked at 2.4 GHz. For double precision floating-point operations, the theoretical peak performances of these platforms are 3741.4 (2×662.4+2×1208.3) Gflop/s and 2877.4 (2×230.4+2×1208.3) Gflop/s, respectively.

This work was supported by the National Science Centre, Poland under grant no. UMO-2015/17/D/ST6/04059. The authors are grateful to the Czestochowa University of Technology for granting access to Intel CPU and Xeon Phi platforms providing by the MICLAB project No. POIG.02.03.00.24-093/13.

Keywords: **Intel Xeon Phi, numerical model of solidification, hybrid architecture, heterogenous programmig model, OpenMP, offload, vectorization**

References

[1] Adrian H., Spiradek-Hahn K., The simulation of dendritic growth in Ni-Cu alloy using the phase field model, Archives of Materials Science and Engineering, 40(2), 89–93, 2009.
[2] Warren J.A., Boettinger W.J., Prediction of dendritic growth and microsegregation patterns in a binary alloy using the phase-field method, Acta Metallurgica et Materialia, 43(2), 689–703, 1995.
[3] Longinova T., Amberg G., Agren J., Phase-field simulations of non-isothermal binary alloy solidification, Acta Materialia, 49(4), 573–581, 2001.
[4] Rojek K.A., Ciznicki M., Rosa B., Kopta P., Kulczewski M., Kurowski K., Piotrowski Z.P., Szustak L., Wojcik D.K., Wyrzykowski R., Adaptation of fluid model EULAG to graphics processing unit architecture, Concurrency and Computation: Practice and Experience, 27(4), 937-957, 2015
[5] Wyrzykowski R., Szustak L., Rojek K., Tomas A., Towards efficient decomposition and parallelization of MPDATA on hybrid CPU-GPU cluster, Lect. Notes in Comp. Sci., 8353, 434–444, 2014.
[6] Szustak L., Rojek K., Wyrzykowski R., Gepner P., Toward efficient distribution of MPDATA stencil computation on Intel MIC architecture, HiStencils'14 Proc. 1st International Workshop on High-Performance Stencil Computations, 51–56, 2014.
[7] Szustak L., Halbiniak K., Kulawik A., Wróbel J., Gepner P., Toward parallel modeling of solidification based on the generalized finite difference method using Intel Xeon Phi, Wyrzykowski, R., Deelman, E., Dongarra, J., Karczewski, K., Kitowski, J., Wiatr, K. (eds.) PPAM 2015, Part I. LNCS, 9573, 411–412, 2016.
[8] Szustak L., Rojek K., Olas T., Kuczyński L., Halbiniak K., Gepner P., Adaptation of MPDATA heterogeneous stencil computation to Intel Xeon Phi coprocessor, Scientific Programming, 14, 2015.
[9] Pilot Laboratory of Massively Parallel Systems (MICLAB), http://miclab.pl.

NUMERICAL ANALYSIS OF MECHANICAL PROPERTIES OF LUMBAR SPINE IMPLANT FOR L3-L4 SEGMENTS

Aneta Idziak-Jabłońska

Institute of Mechanical Technology, Czestochowa University of Technology, Czestochowa, Poland
idziak-jablonska@iop.pcz.pl

Lifestyles of contemporary humans are characterized by much time spent in the sitting position. According to the statistical data, the main cause of disability of people below 45 years of age is low back pain, with around 75% of the population affected by this problem. Therefore, the aim of the present study was to design the spine implant using the finite element method.
One of the methods to evaluate quality of new structures used at the design stage is computer simulation of mechanical properties (strength). The simulation allows for the analysis of stress and strain using the model that represents spinal segments with an implant. The causes of the damage to the system of tissue and implant are complex and connected with a uniform distribution of stress fields and substantial concentration of stress.

A number of factors should be taken into account in the design of an intervertebral implant. First and foremost, the implant should fit the intervertebral space. Another important requirement is that the implant should ensure mobility consistent with anatomical range of movements while improving the stability of the spinal segment. Other requirements concerning vertebral implant design include its life, strength adjusted to the expected load, reliability, easiness of implantation during surgical intervention and opportunities for replacement if the implant is worn. Mechanical analysis was conducted for the implant design in terms of the choice of the materials for its components. The complete intervertebral implant was composed of the bottom plate, upper plate and an intermediary disc between the plates. Fig. 1 presents the geometry and model of implant after discretization and with the load applied. The design of the implant modelled ensures obtaining the anterior and posterior inclination angles of ±10º, and right and left inclination angles of ±7º, whereas the angle for the rotational movement in the transverse plane was ±12º.

Strength analysis of the implant in the coordinate system x_i, i=1,2,3 was focused on determination of the field of displacements u, strain ε and stress σ with the respective components u_i, ε_{ij}, σ_{ij}, i,j=1,2,3 for specific boundary conditions. These conditions were defined for both displacements (e.g. implant support) and implant stress (load conditions).

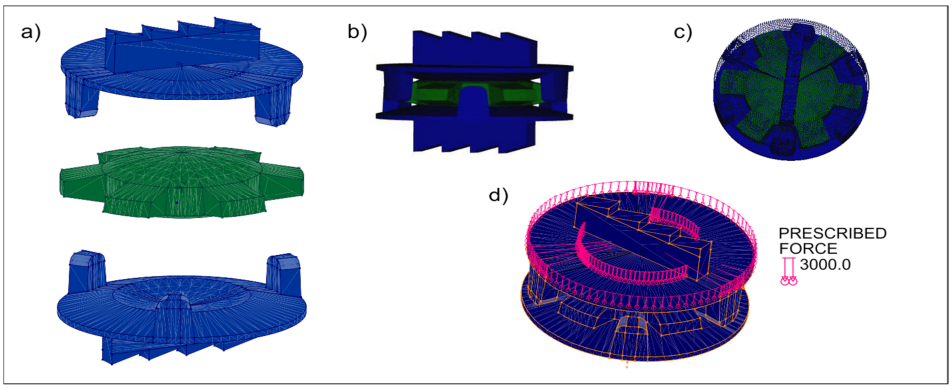

Fig. 1. Implant design: a) exploded view, b) geometrical model, c) isometric view, d) load diagram

In the process of deformation, tensor functions u_i, ε_{ij}, σ_{ij}, i,j=1,2,3 were defined by the following relationships:
- equilibrium equation:

$$\frac{\partial \sigma_{ij}}{\partial x_{ij}} = 0 \tag{1}$$

- continuity equation:

$$\varepsilon_{ij} = \left(\frac{\partial u_i}{\partial x_j} + \frac{\partial u_j}{\partial x_i} \right) = 0 \tag{2}$$

Evaluation of the stress state is based on the reduced (effective) stress.

$$\sigma_{zred}\left(\sigma_{ij}\right) = \sqrt{\frac{3}{2}\left(\sigma_{ij} - \sigma_m\right)\left(\sigma_{ij} - \sigma_m\right)} \tag{3}$$

If the stress state σ_{ij} is determined by the main stress, this condition adopts the following form:

$$\sigma_{zred} = \sqrt{\left(\sigma_1 - \sigma_2\right)^2 + \left(\sigma_1 - \sigma_3\right)^2 + \left(\sigma_2 - \sigma_3\right)^2} \tag{4}$$

During the strength analysis of the implant, the upper and bottom plates were adopted as made of biocompatible metallic materials whereas the disc between the plates was analyzed using the metallic material and various plastics.

Keywords: **biomedical engineering, lumbar spine, implants, FEM**

References

[1] Gzik M., Biomechanika kręgosłupa człowieka. Wyd. Politechniki Śląskiej, Gliwice 2007

FULLY DECENTRALIZED PROTOCOL OF VOTING

Artur Jakubski

Institute of Computer and Information Sciences, Czestochowa University of Technology, Czestochowa, Poland
Institute of Mathematics, Czestochowa University of Technology, Czestochowa, Poland
artur.jakubski@icis.pcz.pl

In many applications, the assumption of unlimited trust to a central authority is difficult or simply impossible to satisfy. The electronic currency Bitcoin protocol is a new motivation for cryptography with no trusted party.

In this paper we propose a secure and efficient voting scheme based on secret sharing, multi-party computation and the Chinese Remainder Theorem. We present fully decentralized protocols for voting as one of the basic computational mechanisms in secure concurrent infrastructure with no trusted party. We adopt the honest-but-curious framework of multiparty computations, executed collectively in a fully decentralized environment of cooperating participants / servers. The discussed protocols form the beginning of our research on applications in the field of multilateral voting problems. Fully distributed or fully decentralized means: with no trusted party whatsoever and with all the parameters shared as a secret. The main idea is that all the input integer parameters are never revealed. Instead, they are shared by participants using an appropriate secret sharing. We are going to use the elementary additive secret sharing but also secret sharing based on Shamir secret sharing and the BGW method. The correctness proofs and analysis of complexity are provided in this paper. Furthermore we present how we will develop this paper.

The paper contains the original project of voting.

Keywords: **multi-party computations, secret sharing, modular arithmetic, voting, e-voting, computational complexity, cryptography**

References

[1] Ben-Or M., Goldwasser S., Wigderson A., Completeness theorems for noncryptographic fault-tolerant distributed computation, STOC, 1988, 1-10.

[2] Blakley G.R., Safeguarding cryptographic keys, Proc. AFIPS 1979, National Computer Conference, AFIPS, 1979, 313-317.

[3] Boneh D., Franklin M., Efficient generation of shared RSA key, Advances in Cryptology-CRYPTO'97, Springer, 1997, v.1296, 425-439.

[4] Chao Ning, Qiuliang Xu, Constant-rounds, linear multiparty computation for exponentiation and modulo reduction with perfect security, In Asiacrypt'11, 2011.

[5] Chun-Pong Lai, Cunsheng Ding, Several generalizations of Shamir's secret sharing scheme, Internat. J. Found. Comput. Sci. 2004, 15, 445-458.

[6] Cocks C., Split knowledge generation of RSA parameters in cryptography and coding, 6th IMA Conference, LNCS, Springer-Verlag, 1997, 1355, 89-95.

[7] Ghodosi H., Pieprzyk J., Steinfeld R., Multi-party computation with conversion of secret sharing, Designs Codes and Cryptography, Springer-Verlag, March 2012, Vol.62, Issue 3, pp. 259-272.

[8] Jakubski A., Selected application of the Chinese Remainder Theorem in multiparty computation, Journal of Applied Mathematics and Computational Mechanics 2016, 15(1), 39-47.

[9] Jakubski A., Perliński R., Review of general exponentiation algorithms, Journal of Applied Mathematics and Computational Mechanics 2011, 10(2), 87-97.

[10] Mignotte M., How to share a secret, in: Advances in Cryptology, Eurocrypt'82, LNCS, volume 149, Springer-Verlag, 1983, pp. 371–375.

[11] Menezes A., van Oorschot P., Vanstone S. A., Handbook of Applied Cryptography, CRC Press, 1999.

[12] Nojoumian M, Stinson D. R., Dealer-Free Threshold Changeability in Secret Sharing Schemes, Cryptology ePrint Archive, Report 2009/268, http://eprint.iacr.org/.

[13] Shamir A., How to share a secret, Communications of the ACM, 22(11), 612-613, 1979.

[14] Spież S., Srebrny M., Urbanowicz J., Remarks on the classical threshold secret sharing schemes, Fundamenta Informaticae 2012, 114 (3-4), 345-357.

MODELLING SMALL OBJECT MOVEMENT IN PORT BASINS USING GRAPH THEORY

Monika Kijewska

Institute of Marine Technologies, Maritime University of Szczecin, Szczecin, Poland
m.kijewska@am.szczecin.pl

Modelling object movement in the water is very complicated issue. It requires the influence of the sea current field, the wind field, and the wave field on the moving object in the water. The effect of these parameters on the object movement is dependent on the degree of its emersion in the water, the type of the object and the type of the water basin, in which the object is located. ([1],[2])

In this paper, the method for modelling the surface current's influence on small objects moving in the port basins will be presented. It is assumed that considered objects are immersed in the water with the exception of at most the part not larger than the human head. As a consequence, the movement of these objects is caused by the surface currents. The influence of the wind field and the wave field is then neglected. The interactions between the surface currents and these objects will be determined by the weighted directed graph [3]. The edge weights of the graph will be defined on the basis on surface current directions generated by the hydrodynamic models. Moreover, the object movement time will be determined based on the surface current speeds.

Thus, the method for modelling surface current influence on small objects immersed in the port basins allows to implement an application supporting the rescue action planning in these basins. Such an application can be used for locating these objects, i.e., survivors, measuring buoys. This approach enables to estimate the route of these objects.

Keywords: **graph theory, sea rescue**

References

[1] Iamsar Manual, International Aeronautical and Maritime Search and Rescue Manual, Mission Co-ordination, International Maritime Organization, 2013, 2.
[2] Pyrcha J., Application of the Fuzzy Set Theory to the Representation of the Visual Information in Support of the Localization of Objects on the Sea Surface, AGH University of Science and Technology Press, Cracow 2008, 184, 93 – 97.
[3] Diestel R., Graph theory, Springer-Verlag New York, Inc, Electronic Edition 2000, GTM 173.

THE INTEGRAL REPRESENTATION OF FELLER SEMIGROUP ASSOCIATED WITH DIFFUSION PROCESS ON A LINE WITH MOVABLE MEMBRANE

Bohdan Kopytko [1], ***Roman Shevchuk*** [2]

[1]*Institute of Mathematics, Czestochowa University of Technology, Czestochowa, Poland*
[2]*Vasyl Stefanyk Precarpathian National University Ivano-Frankivsk, Ukraine*
[1]*bohdan.kopytko@im.pcz.pl,* [2]*r.v.shevchuk@gmail.com*

We consider the problem of construction of the two-parameter semigroup of operators T_{st}, $0 \le s < t \le T$, associated with inhomogeneous Feller process on a line such that in domains $(-\infty, r(s))$ and $(r(s), \infty)$, where $r(s)$ is given function, it coincides with diffusion processes given there by their generating differential operators, and its behaviour after the diffusion particle reaches the common boundary of these domains $r(s)$ is determined by different variants of general (nonlocal) Feller-Wentzell conjugation condition [1]. This problem is also called the problem of pasting together two diffusion processes on a line or the problem of construction of mathematical model of physical phenomenon of diffusion in medium with membrane [2]. To solve the problem we use the analytic methods with an application of classical theory of parabolic potentials. With such an approach, assuming that diffusion characteristics of output diffusion processes are Hölder continuous with respect to both variables and diffusion coefficients are uniformly bounded away from zero, and curve $r(s)$ satisfies Hölder condition with exponent $>1/2$, we obtain the integral representation of desired semigroup as a solution of corresponding conjugation problem for linear parabolic equation of second order with discontinuous coefficients. Note that earlier in [3] the problem of pasting together diffusion processes on a line was studied by the method mentioned above in sufficiently general formulation in case the membrane is placed in a fixed point $r(s) \equiv r_0$.

Keywords: **diffusion process with membrane, potential method, Feller semigroup**

References

[1] Langer H., Schenk W., Knotting of one-dimensional Feller processes, Math. Nachr., 1983, 113, 151-161.
[2] Portenko M.I., Diffusion processes in media with membranes, Proc. of Institute of Mathem. Of National Academy of Sci. of Ukraine, Kyiv, 1995 (in Ukrainian).
[3] Kopytko B., Shevchuk R., On pasting together two inhomogeneous diffusion processes on a line with the general Feller-Wentzell conjugation condition, Theory of Stochastic Processes, 2011, 17(33), 2, 55-70.

FRACTIONAL HEAT CONDUCTION IN A MULTILAYER HEMISPHERE AND SPHERICAL CONE

Stanisław Kukla, Urszula Siedlecka

Institute of Mathematics, Czestochowa University of Technology, Czestochowa, Poland
stanislaw.kukla@im.pcz.pl, urszula.siedlecka@im.pcz.pl

The heat conduction problem in spherical multilayer geometries on the basis of Fourier law has been considered by Jain at all. in paper [1,2]. The subject of this contribution is an analysis of time-fractional heat conduction in an *N*-layered spherical cone and a hemisphere (Fig. 1). The time-fractional heat conduction in spherical coordinate is governed by the differential equation

$$\frac{1}{r^2}\frac{\partial}{\partial r}\left(r^2\frac{\partial T_i}{\partial r}\right)+\frac{1}{\lambda_i}g_i(r,t)+\frac{1}{r^2\sin\varphi}\frac{\partial}{\partial\varphi}\left(\sin\varphi\frac{\partial T_i}{\partial\varphi}\right)=\frac{1}{a_i}\frac{\partial^\alpha T_i}{\partial t^\alpha}, \qquad (1)$$
$$r\in[r_{i-1},r_i],\quad 0<\alpha\le 1,\quad i=1,\ldots,n,\quad 0\le\varphi\le\phi\ \left(\phi\in(0,\pi\rangle\right)$$

where r,φ are spherical coordinates, r_i, λ_i and a_i are outer radius, thermal conductivity and thermal diffusivity of the *i*-th spherical layer, respectively, $T_i(r,t)$ is the temperature in the *i*-th layer and $g_i(r,t)$ is a volumetric energy generation, α denotes fractional order of the Caputo derivative with respect to time *t*.

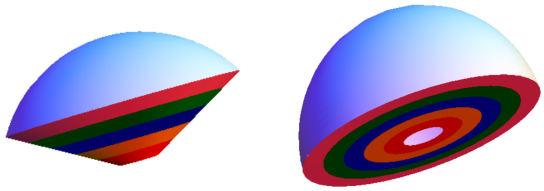

Fig. 1. A schematic diagrams of the *N*-layered spherical cone and hemisphere

The boundary conditions are

$$\lambda_1\frac{\partial T_1}{\partial r}(r_0,\mu,t)=-a_+\left(T_+(\mu)-T_1(r_0,\mu,t)\right) \qquad (2)$$

$$-\lambda_n\frac{\partial T_n}{\partial r}(r_n,\mu,t)=-a_\infty\left(T_\infty(\mu)-T_n(r_n,\mu,t)\right) \qquad (3)$$

$$T_i(r,\mu_\phi,t)=0 \qquad (4)$$

and the conditions of perfect thermal contact between the layers are [3]

$$T_i\left(r_i,\mu,t\right)=T_{i+1}\left(r_i,\mu,t\right),\qquad i=1,...,n-1 \tag{5}$$

$$\lambda_i\frac{\partial T_i}{\partial r}\left(r_i,\mu,t\right)=\lambda_{i+1}\frac{\partial T_{i+1}}{\partial r}\left(r_i,\mu,t\right),\qquad i=1,...,n-1 \tag{6}$$

where a_+, a_∞ are inner and outer heat transfer coefficients and T_+, T_∞ are inner and outer ambient temperatures. The initial condition is assumed in the form

$$T_i\left(r,\mu,0\right)=F_i\left(r,\mu\right) \tag{7}$$

An exact solution of the problem of the time-fractional heat conduction for $g_i\left(r,t\right)=0$ can be presented in the form of eigenfunctions series

$$T_i\left(r,\mu,t\right)=\sum_{m=1}^{\infty}\left(\varphi_{im}\left(r\right)+\sum_{k=1}^{\infty}R_{ikm}\left(r\right)\Lambda_{km}\left(t\right)\right)P_{\beta_m}\left(\mu\right) \tag{8}$$

where $\varphi_{im}\left(r\right)=C_{i1}r^{\beta_m}+C_{i2}r^{-\beta_m-1}$, $R_{ikm}\left(r\right)=B_{i1}j_{\beta_m}\left(\omega_{ikm}r\right)+B_{i2}y_{\beta_m}\left(\omega_{ikm}r\right)$,

$\Lambda_{km}\left(t\right)=\dfrac{1}{N_{km}^{r}N_{m}^{\mu}}E_{\alpha,1}\left(-\gamma_{km}^{2}t^{\alpha}\right)\sum_{i=1}^{n}\dfrac{\lambda_i}{a_i}\int_{r_{i-1}}^{r_i}r^2R_{ikm}\left(r\right)\int_{1}^{\mu_\phi}\Psi_m\left(\mu\right)F_i^{*}\left(r,\mu\right)d\mu dr$,

j_{β_m}, y_{β_m} are spherical Bessel functions and E_α is the Mittag-Leffler function.

Using the solution (8), the temperature distribution in the spherical cone (or hemisphere) for different values of the order $0<\alpha\le 1$ can be numerically determined. The solution can be used to analysis of fractional heat conduction in a continuously graded body in spherical coordinates.

Keywords: **time-fractional heat conduction, multilayered spherical cone**

References

[1] Jain P.K., Singh S., Rizwan-uddin, An exact solution for two dimensional, unsteady, multilayer heat conduction in spherical coordinates, International Journal of Heat Mass Transfer 53, 2010, 2133-2142.

[2] Siedlecka U. Radial heat conduction in a multilayered sphere, Journal of Applied Mathematics and Computational Mechanics 13(4), 2014, 109-116.

[3] Povstenko Y., Time-fractional heat conduction in an infinite medium with a spherical hole under Robin boundary condition, Fractional Calculus and Applied Analysis, 16(2), 2013, 354-369.

THE ROLE OF THE ANISOTROPY OF THE MESH IN THE MODELING OF SOLIDIFICATION

Adam Kulawik

Institute of Computer and Information Sciences, Czestochowa University of Technology, Czestochowa, Poland
adam.kulawik@icis.pcz.pl

In the paper the impact of the regularity of distribution of compute nodes on the results of the simulation of two-component alloy solidification is analyzed. The solidification of Ni-Cu alloy is considered. It is characterized by the formation of ideal solutions in both the liquid and solid state, and an equilibrium phase diagram of the system is unlimited solubility of components in the solid state.

The considered process is a dendritic solidification in the isothermal conditions with constant diffusivity coefficients for the solid or liquid phases. For the analysis the phase field method defined by Warren and Boettinger was applied [1,2,3].

In this method, the growth of microstructure during solidification is determined by solving a system of two differential equations - the content of the solid phase (1) and the concentration of the dopant (2) in the analyzed area.

$$\begin{aligned}\varphi_i^{t+1} = \varphi_i^t + \Delta t M_\varphi \bar{\varepsilon}^2 \Bigg[\eta^2 \left(\frac{\partial^2 \varphi_i^t}{\partial y^2} + \frac{\partial^2 \varphi_i^t}{\partial x^2} \right) + \eta\eta' \Bigg(\sin\left(2\theta - \theta_0\right) \left(\frac{\partial^2 \varphi_i^t}{\partial y^2} - \frac{\partial^2 \varphi_i^t}{\partial x^2} \right) + \\ +2\cos\left(2\theta - \theta_0\right) \frac{\partial^2 \varphi_i^t}{\partial x \partial y} \Bigg) - 0.5\left(\eta'^2 + \eta\eta''\right) \Bigg(2\sin\left(2\theta - \theta_0\right) \frac{\partial^2 \varphi_i^t}{\partial x \partial y} + \\ -\cos\left(2\theta - \theta_0\right) \left(\frac{\partial^2 \varphi_i^t}{\partial y^2} - \frac{\partial^2 \varphi_i^t}{\partial x^2} \right) - \frac{\partial^2 \varphi_i^t}{\partial x^2} - \frac{\partial^2 \varphi_i^t}{\partial y^2} \Bigg) \Bigg] + \\ +\Delta t M_\varphi \left(-cH_B - \left(1 - c\right) H_A - cor \right)\end{aligned} \tag{1}$$

where: M_ϕ is defined as the solid/liquid interface mobility, $\bar{\varepsilon}$ is a parameter related to the interface width, η is the anisotropy factor, H_A and H_B denotes the free energy of both components, cor is the stochastic factor which models thermodynamic fluctuations near the dendrite tip, θ is the function of derivatives of ϕ, θ_0 is rotation degree of structure.

$$
\begin{aligned}
c_i^{t+1} = c_i^t + \Delta t \Bigg\{ & \frac{\partial D_c}{\partial x}\left[\frac{\partial c_i^t}{\partial x} + \frac{V_m}{R} c_i^t\left(1-c_i^t\right)\left(H_B - H_A\right)\frac{\partial \phi_i^t}{\partial x}\right] + \\
& + D_c\left[\frac{\partial^2 c_i^t}{\partial x^2} + \frac{V_m}{R}\left[\left(1-2c_i^t\right)\frac{\partial c_i^t}{\partial x}\left(H_B - H_A\right)\frac{\partial \phi_i^t}{\partial x} + \right.\right. \\
& \left.\left. + c_i^t\left(1-c_i^t\right)\frac{\partial\left(H_B - H_A\right)}{\partial x}\frac{\partial \phi_i^t}{\partial x} + c_i^t\left(1-c_i^t\right)\left(H_B - H_A\right)\frac{\partial^2 \phi_i^t}{\partial x^2}\right]\right] + \\
& + \frac{\partial D_c}{\partial y}\left[\frac{\partial c_i^t}{\partial y} + \frac{V_m}{R} c_i^t\left(1-c_i^t\right)\left(H_B - H_A\right)\frac{\partial \phi_i^t}{\partial y}\right] + \\
& + D_c\left[\frac{\partial^2 c_i^t}{\partial y^2} + \frac{V_m}{R}\left[\left(1-2c_i^t\right)\frac{\partial c_i^t}{\partial y}\left(H_B - H_A\right)\frac{\partial \phi_i^t}{\partial y} + \right.\right. \\
& \left.\left. + c_i^t\left(1-c_i^t\right)\frac{\partial\left(H_B - H_A\right)}{\partial y}\frac{\partial \phi_i^t}{\partial y} + c_i^t\left(1-c_i^t\right)\left(H_B - H_A\right)\frac{\partial^2 \phi_i^t}{\partial y^2}\right]\right] \Bigg\}
\end{aligned}
\tag{2}
$$

where: D_c is the diffusion coefficient, V_m is the specific volume, R is the gas constant.

To solve the differential equations the generalized finite difference method was used [4]. Therefore anisotropy of the grid may be the result not only of the discretization of region but also the links between the nodes of the mesh.

Because the computation in the explicit scheme is performed the parallel calculation was used. The number of unknown variables was divided symmetrically between the computational nodes. The values of derivative in the nodes (1, 2) are determined at every step of calculations. They are a main factor which influence on the CPU load. The computation in the equations (1) and (2) have been implemented with using the Intel Xeon Phi architecture [5].

The paper presents the results of calculations for the development of a single grain in the control region of the liquid phase of the shape of a square 69×69 μm and the growth time equal 1ms with assumed value of supercooling of liquid. Several types of grid nodes were considered. In the first case, the calculation was carried out (fig. 1) for a regular grid constructed with square units for different values of the parameter of width of the solidification front. From the assumptions of the method imply, that the width of a solidification front must be greater than the distance between the nodes of grid. The results of the calculations show that limitation for the selected numerical method is the distance in the value of derivatives between neighboring nodes for a single node.

The second case was the comparison of the calculation results (fig. 2) for the same process parameters and the grid nodes rotated by 45 degrees.

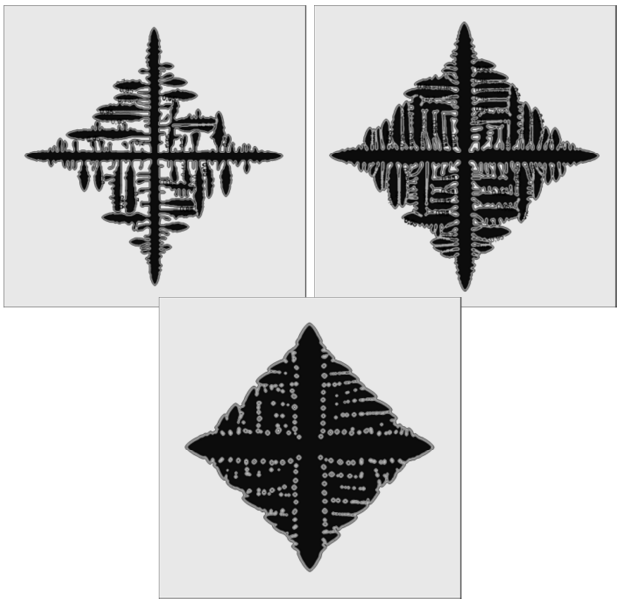

Fig. 1. The shape of the solidified region for different values of the width of front a) 0.8δ b) 1.0δ c) 2.0δ

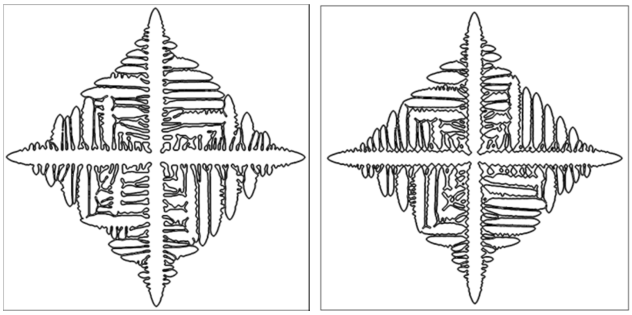

Fig. 2 The boundaries of the solidified region a) uniform square mesh, b) a uniform square mesh rotated through 45 degrees

For these conditions of simulations differences in the obtained results are noticeable, particularly visible in the growth areas of secondary dendrite branches. It can also be observed in the width of the primary branch. In the third case the calculations (fig. 3) are performed for the regular mesh but different distances between the computational nodes for the x and y directions.

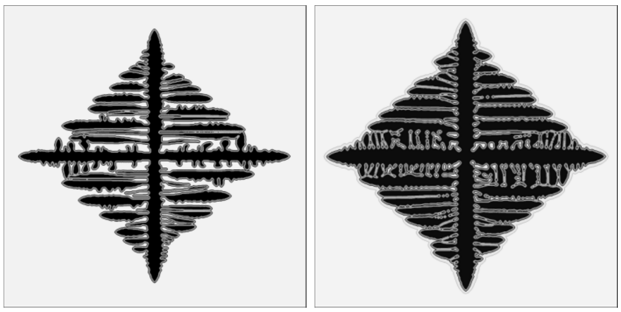

Fig. 3. The shape of the solidified region for grid $\Delta y = 1.2\Delta x$ a) 2000x2000 mesh nodes, b) 2500x2500 mesh nodes

On the basis of obtained results can be concluded (for the presented model) that there is a strong dependence of the solid phase growth not only on the anisotropy of the grid but also on its density. All of the above examples of calculations were carried out with the assumption that to determine the value of derivatives the nearest eight nodes for GFDM are needed. Taking into account only six of them lead, for the structural grids to degeneration of the results (fig. 4).

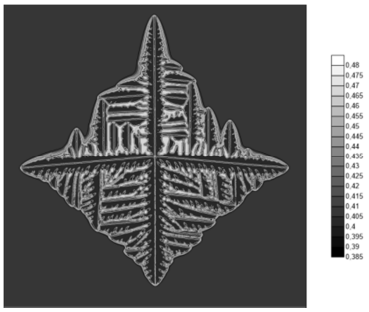

Fig. 4. Dopant concentration - inclusion in the model of 6 neighbouring nodes

The simulation results for the dendritic solidification process show a strong dependence of the results, in the presented model, on the parameters of method for determining the derivative and a strong influence of the deployment of compute nodes.

Keywords: **numerical methods, computational mechanics, phase field model, solidification, generalized finite difference method, anisotropy of mesh**

References

[1] Adrian H., Spiradek-Hahn K., The simulation of dendritic growth in Ni-Cu alloy using the phase field model, Archives of Materials Science and Engineering, 2009, 40 (2), 89–93.
[2] Warren J.A., Boettinger W.J., Prediction of dendritic growth and microsegregation patterns in a binary alloy using the phase-field method, Acta Metallurgica et Materialia, 1995, 43 (2), 689–703.

[3] Longinova T., Amberg G., Agren J., Phase-field simulations of non-isothermal binary alloy solidification, Acta Materialia, 2001, 49 (4), 573–581.
[4] Benito J.J., Uren F., Gavete L., The Generalized Finite Difference Method, In: Leading-Edge Applied Mathematical Modeling Research, ed. Alvarez M.P., Nova Science Publishers, Inc., 2008.
[5] Szustak L., Halbiniak K., Kulawik A., Wrobel J., Gepner P., Toward parallel modeling of solidification based on the generalized finite difference method using Intel Xeon Phi, Wyrzykowski R., Deelman E., Dongarra J., Karczewski K., Kitowski J., Wiatr K. (eds.) PPAM 2015, Part I. LNCS, 2016, 9573, 411–412.

DETECTION AND TRACKING OF THE CHARACTERISTICS FEATURES FOR THE OBJECTS ON SATELLITE IMAGE

Joanna Kulawik

Institute of Computer and Information Sciences, Czestochowa University of Technology, Czestochowa, Poland
joanna.kulawik@icis.pcz.pl

The modern technology allows obtaining multiple digital images with excellent quality. The value of image information is contained in them. Access to this information is possible through the processing and analysis of digital images obtained from different types of devices. Image processing involves the transformation of that it became possible to obtain the specific characteristics of the test image. The best effects of such actions are obtained considering each image individually, but it is time consuming.

Image processing requires the use of detection of the characteristics features. Depending on how the image was captured, different methods and functions of the detection characteristics may be used.

This article will explain how to detect them in the images of Earth from the aerial new. To simplify the calculation the images are converted to grayscale. In order to suppress the noise which often appears on this type of images there will be used convolution matrix mask with 2-dimensional matrix, discrete image [1] written by the following formula:

$$I_2(x,y) = \sum_{p,q \in MF} I_1(x-p, y-q) w(p,q) \tag{1}$$

where:
I_1 – input image matrix, I_2 – image matrix obtained after filtration,
$w(p,q)$ – mask (matrix) of the filter.

Performing the above mentioned filtration requires the use of normalization [1], which is described by the following equation:

$$I_3(x,y) = \frac{I_2(x,y) - \min(I_2(x,y))}{\max(I_2(x,y)) - \min(I_2(x,y))} 2^B \tag{2}$$

where:
I_2 – image matrix obtained after filtration,
I_3 – image matrix obtained after normalization,
B – is the number of bits representing the pixel.

To detect characteristic features which are the corners Harris and Stephens [2] method will be used. This is one of many corner detection algorithms, Which is defined by :

$$E(u,v) = \sum_{x,y} w(x,y)[I(x+u, y+v) - I(x,y)]^2 \tag{3}$$

where:
$w(x,y)$ – mask (matrix) of the filter.

Objects in the input image are detected by using a detector surface Speeded-Up Robust Features (SURF) [3] described by the following formula:

$$H(p,\sigma) = \begin{pmatrix} L_{xx}(p,\sigma) & L_{xy}(p,\sigma) \\ L_{xy}(p,\sigma) & L_{yy}(p,\sigma) \end{pmatrix} \tag{4}$$

where:
$L_{xx}(p,\sigma)$ etc. – second – order derivatives of the grayscale image,
$p=(x,y)$ – point in a image I,
$H(p,\sigma)$ – hessian matrix at point p and scale σ.

Regions is another characteristic of the image used for the detection of stable areas in the paintings depicting different points of view. Detection of regions will be carried out using the method Maximally Stable Extremal Region (MSER). For MSERs we only Consider extremal regions [4] Which are defined by:

$$\forall p \in R_i, \forall q \in boundary\,(R_i) \rightarrow I(p) \geq I(q) \tag{5}$$

where:
I – imput image,
R_i – extremal regions.

In this presentation of the previously mentioned characteristic features, there will be used photos of the surrounding area of Czestochowa, derived from the Internet.

Fig. 1. Example of the image subjected to detection characteristics of size 1536 x 768.

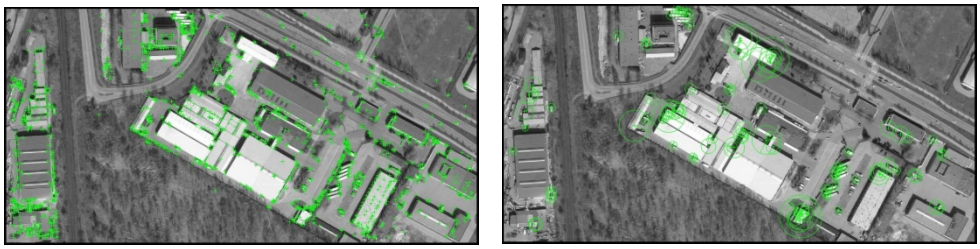

Fig. 2. The detection of characteristics features: the left by Harris and Stephens; to the right by Speeded-Up Robust Features (SURF).

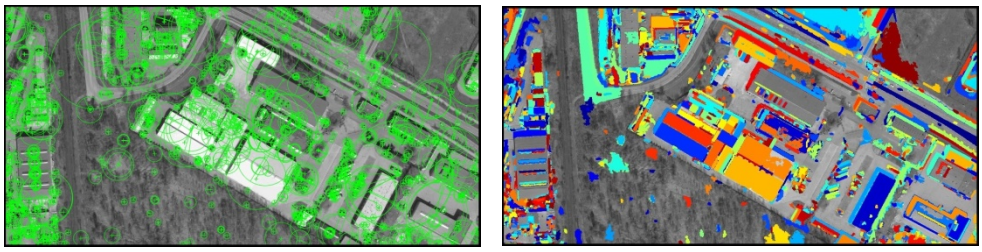

Fig. 3. The detection of characteristics features the method by Maximally Stable Extremal Region (MSER).

Fig. 4. Examples of images subjected to detection of size 768 x 512 pixels.

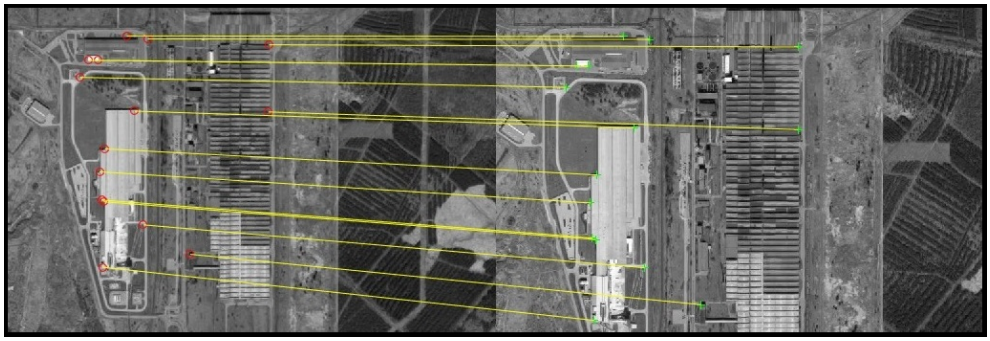

Fig. 5. Example of detection corners by Harris and Stephens.

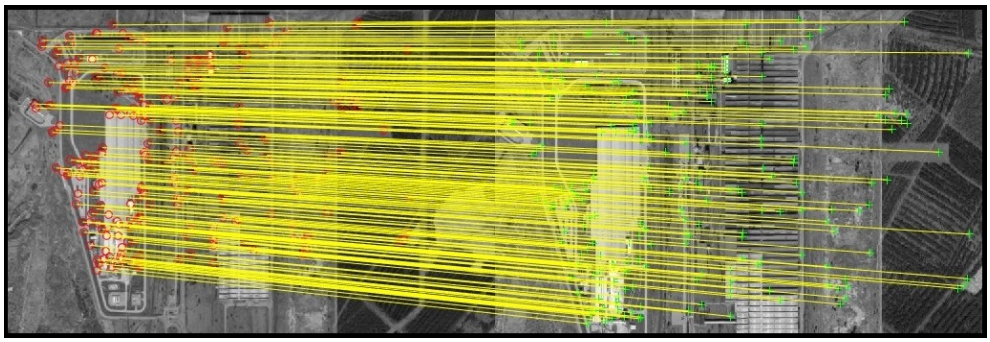

Fig. 6. Example of detection objects by Speeded-Up Robust Features (SURF).

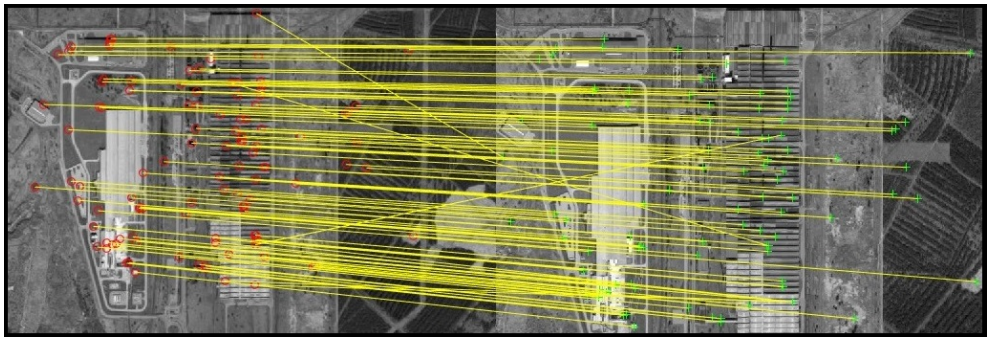

Fig. 7. Example of detection regions by Maximally Stable Extremal Region (MSER).

Keywords: **corner detection, detection Harris, feature detection SURF, detection MSER**

References

[1] Tadeusiewicz R., Korohoda P., Komputerowa analiza i przetwarzanie obrazów, Wydawnictwo Fundacji Postępu Telekomunikacji, Kraków, 1997.
[2] Harris C., Stephens M., A combined corner and edge detector, Proceedings of the 4th Alvey Vision Conference, 1988, 147–151.
[3] Bay H., Ess A., Tuytelaars T., Van Gool L., Speeded Up Robust Features, ETH Zurich, Katholieke Universiteit Leuven, 2008.
[4] Donoser, M., Bischof, H., Efficient Maximally Stable Extremal Region (MSER) Tracking CVPR, 2006.

IMPLICATIONS OF CONSIDERING PSEUDOGROUPS OF TRANSFORMATIONS ON DISCRETE AND ANTIDISCRETE TOPOLOGICAL SPACES

Jolanta Lipińska

Institute of Mathematics, Czestochowa University of Technology,
Czestochowa, Poland
jolanta.lipinska@im.pcz.pl

In the earlier papers we considered pseudogroups of transformations on discrete and antidiscrete topological spaces. The problem which appears is what are implications of considering such extraordinary cases as in applications we rather deal with pseudogroups on real number space with natural topology or in case of need pseudogroups on complex number space. There are two theorems which shows it is worth of considering.
First theorem is connected with pseudogroups on antidiscrete topological spaces. It says that every group of transformation can be considered as a pseudogroup of transformations on an antidiscrete topological space. Let us recall the following definition introduced in [1].

Definition. *A non-empty set* Γ *of functions, for which domains* D_f *are arbitrary non-empty sets, will be called a pseudogroup of functions if it satisfies the following conditions:*

1° $\quad f\left(D_f\right)\cap D_g \neq \varnothing \Rightarrow g\circ f \in \Gamma$ *for* $f,g\in\Gamma,$

2° $\quad f^{-1}\in\Gamma$ *for* $f\in\Gamma,$

3° $\quad \bigcup\Gamma'\in\Gamma$ *for* $\Gamma'\in\langle\Gamma\rangle$

where

$$\langle\Gamma\rangle=\left\{\varnothing\neq\Gamma'\subset\Gamma\ :\ \bigcup\Gamma' \text{ is a function and } \bigcup\left(\Gamma'\right)^{-1} \text{ is a function}\right\}$$

and

$$\left(\Gamma'\right)^{-1}=\left\{f^{-1}\ :\ f\in\Gamma'\right\}$$

and f^{-1} *denotes an inverse relation.*

As we consider this definition we can simply say that every group of transformations is a pseudogroup of functions. It means that notion of a pseudogroup of functions is generalization of a notion of a group of transformations.

The second theorem is connected with pseudogroups on discrete topological spaces. It says that if a generalized inverse semigroup is isomorphic with a pseudogroup of transformations on a discrete topological spacer then for any idempotent exists smaller or equal to it idempotent for which does not exist smaller idempotent.

Keywords: **pseudogroups of transformations**

References

[1] Lipińska J., Diffeomorphisms of quasi-algebraic spaces, Demonstratio Mat. 19(1986), 139-151.
[2] Lipińska J., Pseudogroups of transformations on discrete topological spaces, Journal of Applied Mathematics and Computational Mechanics, 2016 (in print)
[3] J. Lipińska, Groups of transformations as pseudogroups of functions, Prace Naukowe Instytutu Matematyki i Informatyki, Politechnika Częstochowska, 1(5) 2006

ON A CERTAIN PROPERTY OF GENERALIZED HÖLDER FUNCTIONS

Maria Lupa

Institute of Mathematics, Czestochowa University of Technology
Częstochowa, Poland

We recall the definition of the space $W_\gamma[a,b]$.

Let $[a,b]$ be a closed interval, where $a,b \in R,\ a<b,\ d \coloneqq b-a$. We assume that the following condition is fulfilled

$$(\Gamma)\ \gamma\colon [0,d] \to [0,\infty) \text{ is increasing and concave, } \gamma(0)=0,$$
$$\lim_{t\to 0^+}\gamma(t)=\gamma(0),\ \lim_{t\to d^-}\gamma(t)=\gamma(d).$$

Definition 1.

Denote by $W_\gamma[a,b]$ the set of all *r*-times differentiable functions, where $r \in N$, defined on the interval $[a,b]$ with values in R, such that their *r*-th derivatives satisfy the following condition: there exists a constant $M \geq 0$ such that

$$\left|\varphi^{(r)}(x)-\varphi^{(r)}(\bar{x})\right| \leq M\gamma(|x-\bar{x}|),\ \bar{x},x \in [a,b] \tag{1}$$

where γ fulfils condition (Γ).

The functions of the form $\gamma(t)=t^\alpha$, where $0<\alpha<1,\ t\in[0,d]$, fulfil the assumption (Γ) and moreover $\gamma'_+(0)=+\infty$. Therefore the condition (1) is called *the generalized Hölder condition* or the $\gamma-$*Hölder condition.*

The space $W_\gamma[a,b]$ with the norm

$$\|\varphi\| \coloneqq \sum_{k=0}^{r}\left|\varphi^{(k)}(a)\right| + sup\left\{\frac{|\varphi^{(r)}(x)-\varphi^{(r)}(\bar{x})|}{\gamma(|x-\bar{x}|)};\ x,\bar{x}\epsilon[a,b], x\neq\bar{x}\right\}$$

is a real normed vector space. Moreover, it is a Banach space.

Consider the functional equation

$$\varphi(x)=h(\varphi[f(x)])+g(x)$$

We assume that the given functions the following conditions fulfil

(i) $f\epsilon W_\gamma(I),\ \sup_I|f'|\leq 1$

(ii) $g\colon I\to R,\ \ g\epsilon W_\gamma(I)$.

(iii) $h\colon R\to R$ is C^r class and $h^{(r)}$ fulfils the Lipschitz condition in R.

We define functions $h_k: I \times R^{k+1} \to R, k = 0,1, \dots, r$ by the formula

$$\begin{cases} h_0(x, y_0) := h(y_0) + g(x) \\ h_{k+1}(x, y_0, \dots, y_{k+1}) := \frac{\partial h_k}{\partial x} + f'(x)\left(\frac{\partial h_k}{\partial y_0} y_1 + \dots + \frac{\partial h_k}{\partial y_k} y_{k+1}\right) \end{cases} \tag{2}$$

for $k = 0,1, \dots, r-1$.

Lemma 1.

If the assumptions (i)-(iii) are fulfilled, then the functions h_k defined by (2) are of the form:

1. for $r = 1$

$$h_1(x, y_0, y_1) = h'(y_0) y_1 f'(x) + g'(x); \tag{3}$$

2. for $r \geq 2,\ k = 2, \dots, r$

$$h_k(x, y_0, \dots, y_k) = p_k(x, y_0, \dots, y_{k-1}) + h'(y_0) y_k \left(f'(x)\right)^k +$$

$$+ h'(y_0) y_1 f^{(k)}(x) + g^{(k)}(x) \tag{4}$$

where

$$p_k(x, y_0, \dots, y_{k-1}) + h'(y_0) y_k \left(f'(x)\right)^k =$$

$$= \sum_{i=1}^{k} h^{(k-i+1)}(y_0) \sum_{\alpha_1 + \dots + \alpha_i = k-i+1} u_{\alpha_1 \dots \alpha_i, k}(x) {y_1}^{\alpha_1} \dots {y_i}^{\alpha_i} \tag{5}$$

and the functions $u_{\alpha_1 \dots \alpha_i, k}$ are of the class C^{r-k+1} in I, for all possible natural numbers $\alpha_1, \dots, \alpha_i$ such that $\alpha_1 + \dots + \alpha_i = k - i + 1, k = 2, \dots, r,\ i = 1, \dots, k,$ (some of these functions are identically equal to zero).

References

[1] Lupa M., A special casemof generalized Hölder functions, Journal of Applied Mathematics and Computational Mechanics, V 13, Issue 4(2014) pp.81-89.

[2] Kuczma M., Functional Equations in a Single Variable, PWN, Warszawa 1968.

[3] Kuczma M., Choczewski b., Ger R., Iterative Functional Equations, Cambridge University Press, Cambridge-New York-Port Chester-Melbourne-Sydney 1990.

HIGH PERFORMANCE NUMERICAL COMPUTING IN C++X11

Grzegorz Michalski , Andrzej Grosser

Institute of Computer and Information Sciences, Czestochowa University of Technology, Czestochowa, Poland
grzegorz.michalski@icis.pcz.pl, andrzej.grosser@icis.pcz.pl

Issues appear before engineers currently, require often perform very complex computer simulations on the basis of which can be introduced various kinds of changes to the analysed object (its geometric model). In a significant part of these simulations are calculated distributions of various physical quantities such as stresses, deformations, displacements and temperature. The computation of such distributions for a continuous object in the real space it is only possible in the approximate, by using of the numerical model contemplated phenomenon or physical processes. The numerical model is obtained by solving partial differential equations. These equations make up the mathematical model of the problem being studied. Analytical solution of the generated equations for the problems faced before the engineers in this time is in practice impossible. This is due to the fact that analysed objects usually have complex shapes and are imposed on them complicated boundary conditions.

The most widely used in engineering simulations is discretization of the analysed area, that is, its division into smaller, geometrically simple areas. Discretization of the considered area is used to transform a mathematical model of the issues on its numerical model [1,2]. The final result of this is a system of algebraic equations (usually linear) with a finite numbers of unknowns.

Most frequently for solving of the resulting equations are used modern multicore architectures such as a graphics processors. Programming graphics devices is not easy and requires from the programmer to additionally knowledge about the hardware architecture. An effort associated with the adaptation of the algorithm to a multi-core architectures are not always profitable.

The new standard of the C ++ x11 language is introduced of many facilities [3,4]. To the language was introduced build-in threads to perform computations in parallel on multiple cores. Furthermore, the r-references and a move semantics increased productivity programs. The language has also become easier to learn and use.

They also support the implementation of numerical algorithms for general purpose processors while maintaining an expected high performance of the computation.

The authors of the work has focused on the new elements of the C ++ language that can be used in the implementation of the computer simulations of the physical processes based on PCs.

Keywords: **numerical computing, numerical modelling, high performance, C++x14, parallel computing**

References

[1] Kleiber M. (red.), Komputerowe metody mechaniki ciał stałych, Wydawnictwa Naukowe PWN, Warszawa, 1995
[2] Michalski G., Sczygiol N., Budowa globalnej macierzy sztywności w metodzie elementów skończonych z zastosowaniem procesorów wielordzeniowych, Metody Informatyki Stosowanej, nr 2/2010 (23), p. 92-104
[3] Stroustrup B., Język C++. Kompendium wiedzy, Helion, 2014
[4] Meyers S., Effective Modern C++42 Specific Ways to Improve Your Use of C++11 and C++14, O'Reilly, 2014

COALGEBRAS AS MATHEMATICAL CONSTRUCTION FOR MODELING OBSERVABLE BEHAVIOR

Valerie Novitzka, William Steingartner

Faculty of Electrical Engineering and Informatics, Technical University in Košice
Košice, Slovakia
valerie.novitzka@tuke.sk, william.steingartner@tuke.sk

Abstract: The aim of programming is to force a computer to execute some actions so that we get the expected behavior. The basic idea of behavioral theory is to determine a relation between internal, hidden states and their observable properties. In our contribution we sketch the main ideas of describing behavior of systems by coalgebras.

1. INTRODUCTION

The development of computers has contributed to the development of investigating dynamical features of formal structures. The dynamics involves a state of afairs which can be possibly observed and modified. We can consider the computer state as the combined contents of all memory cells. A user can observe only a part of this state, e.g. on display and he can modify this state by typing commands. As a reaction the computer displays certain behavior. The aim of programming is to force the computer to execute some actions and to generate expected behavior. This behavior can be positive, e.g. desired behaviour; or negative, e.g. side effects that must be excluded from the system. To describe the behavior of a computer system is a non-trivial matter. But some formal description of such complex systems are needed when we wish to reason formally about their behavior. This reasoning is required to achieve the correctness or security of these systems.

The basic idea of behavioral theory is to determine a relation between internal states and their observable properties. The internal states are often hidden. Computer scientists have introduced many formal structures to capture the state-based dynamics, e.g. automata, transition systems, Petri nets, etc. In [2] the notion of behavior in the algebraic specifications was firstly introduced.

2. ALGEBRAS AND COALGEBRAS IN COMPUTER SCIENCE

The execution of a computer program causes generation of some behavior that can be observed typically as computer's input and output. There are also programs changing the internal state of computer that do not produce outputs, e.g. the programs running infinitely, sleeping processes in operating systems which weak up and work only in the case some event occurs. We are also interesting in their

behavior that can be observed using coalgebras. A program can be considered as an element of the (initial) algebra arising from the used programming language. In other words, it is an inductively defined set P of terms. This set forms a suitable algebra

$$F(P) \to P$$

where F is a polynomial endofunctor constructed over the signature of the operations appointed for execution by a program.
Each language construct corresponds to certain dynamics captured in coalgebras. The behavior of programs is described by a (final) coalgebra

$$P \to G(P)$$

where the functor G captures the kind of behavior that can be observed. In other words, generated computer behavior amounts to the repeated evaluation of a (coinductively defined) coalgebraic structure on an algebra of terms. Thus coalgebraic behavior is generated by an algebraic program. Therefore the algebras are used for constructing basic structures used in computer programs and coalgebras acting on the state space on the computer describe what can be observed externally. The relationship between algebras and coalgebras can be regarded as duality. A data type is completely determined by its constructors, algebraic operations going *into* data type. The state can be observed via the visible values and can be modified. In coalgebra it is realised by using destructor operations pointing *out* of the structure.

Coalgebra can be recognized as the study of the states, their operations and properties. States can be imagined as a blackbox to which we have only limited access. The essence of the coalgebraic behavioral theory is the tension between what is actually inside and what can be observed externally.

3. BASIC CONCEPTS

Coalgebraic concept is based on category theory [3,4]. A *category* $\boldsymbol{C}$ is a mathematical structure consisting of *objects*, e.g. $A, B, \ldots$ and *morphisms* of the form $f: A \to B$ between them. Every object has its identity morphism $id_A: A \to A$ and morphisms are composable. Because the objects of a category can be arbitrary structures, categories are useful in computer science, where we often use more complex structures not expressible by sets. Morphisms between categories are called *functors*, e.g. a functor $F: \boldsymbol{C} \to \boldsymbol{D}$ from a category $\boldsymbol{C}$ to a category $\boldsymbol{D}$ which preserves the structure. In this contribution we use only the category ***Set*** with sets as objects and functions between them as morphisms, but this approach can be extended to categories of arbitrary complex objects.

The starting notion in coalgebraic approach is a *signature* used in the theory of algebraic specifications [1]. A signature Σ consists of *types*, e.g. σ, τ, … and *operation symbols* of the form $f: \sigma_1, ..., \sigma_n \to \tau$. In a signature we distinct

- *constructor operations* defined inductively. They tell us how to generate (algebraic) data elements;
- *destructor operations*, also called observers or transition functions defined coinductively. They tell us what we can observe about our data elements;
- *derived operations* that can be defined inductively or coinductively.

If we define a derived operation f inductively, we define the value of f on all constructors. In a coinductive definition of derived operation f we define the values of all destructors on each outcome $f(x)$.

4. COALGEBRA AS OBSERVATION

For a polynomial endofunctor F introduced in the previous section, an F-coalgebra is a pair

$$\langle U, c \rangle$$

where U is a set called *state space* and $c: U \to F(U)$ is the *coalgebraic structure* or operation of the coalgebra $\langle U, c \rangle$. The difference between F-algebra and F-coalgebra is the same as between construction and observation. While F-algebra tells us how to construct elements in the carrier set by the algebraic structure $a: F(U) \to U$ going *into* U, in the case of coalgebra, the coalgebraic operation $c: U \to F(U)$ goes *out* of U. In coalgebras we do not know how to form the elements of U, we have only the operations working on U, which may give some information about U [5]. Therefore, we have only limited access to the state space. F-coalgebras are also models of the corresponding signatures, but instead of the case of F-algebras, these coalgebras are based on destructor operations. A coalgebraic structure is a tuple of functions (destructors) [6]

$$c = \langle destr_1, ...destr_n \rangle : U \to F(U).$$

Example: Consider the signature for data type stack. It specifies type S for stacks and type I for items of stacks. Signature for stack has two destructor operatios

$$pop : S \to S$$
$$top : S \to I$$

where *top* returns a top element of a stack and *pop* removes a top element from top of stack. If a stack is empty, the operation *top* returns nothing. S can be considered as a state space, objects of a category of states. These operations generate polynomial endofunctor $F : S \to S$ defined by

$$F(S) = 1 + S \times I,$$

where 1 denotes an empty stack. Corresponding coalgebraic structure is then the pair of operations

$$\langle pop, top \rangle : S \to 1 + S \times I$$

and *F*-coalgebra is a structure

$$\langle S, \langle pop, top \rangle \rangle .$$

In other words, S is the state space and we can observe the change of states via observable values from *I*. By repeating execution of the operations *pop* and *top* we get a sequence of observable values

$$(i_1, i_2, ..., i_n), \quad \text{for some } n \in N$$

of elements of a stack and a sequence of not observable states

$$(s_1, s_2, ..., new),$$

where the last member of this sequence is the empty stack. The sequence of elements of I is only what we can observe about the whole process. We see that we can get observable values of data structure not at once but *step by step* after repeated application of the operations *top* and *top*.

5. CONCLUSION

In this short contribution we presented the main ideas of coalgebraic approach of behavioral theory. On a simple example of data structure stack we illustrated how the signature's destructor operations induce polynomial endofuctor that is the basic concept in coalgebraic approach. In our future research we extend this approach to some paradigmas of programming including concurrent processes and object-oriented programming.

Acknowledgment

This work was supported by Grant No. FEI-2015-18: Coalgebraic models of component systems.

Keywords: **behavioral theory, coalgebra, category theory**

References

[1] Ehrig H., Mahr B., Fundamentals of algebraic specification 1: Equations and Initial Semantics, EATCS Monographs on Theoretical Computer Science, 1985
[2] Reichel H., Behavioural equivalence - a unifying concept for initial and final specifications, 3rd Hungarian Computer Science Conference, Akadémia kiadó, 3, 1981
[3] Jacobs B., Introduction to coalgebra. Towards mathematics of states and observations (draft), 2005
[4] Jacobs B., Rutten J., A tutorial on (co)algebras and (co)induction, Bulletin of the European Association for Theoretical Computer Science, (62)1997, 222-259
[5] Novitzká V., Mihályi D., Steingartner W., Coalgebraic behaviour of algebraic programs, Analele Universitatii din Oradea, Proc. 8th International Conference on Engineering of Modern Electric Systems,University of Oradea, Romania, (9), 2007, 60-64
[6] Rutten J., Universal coalgebra: a theory of systems, Technical Report CS-R9652, CWI, Amsterdam, 1996

THE EXAMPLES OF NON-KELLER MAPPINGS

***Edyta Pawlak*[1], *Sylwia Lara-Dziembek*[1], *Grzegorz Biernat* [1], *Magdalena Woźniakowska* [2]**

[1]*Institute of Mathematics, Czestochowa University of Technology, Czestochowa, Poland*
edyta.pawlak@im.pcz.pl, sylwia.lara@im.pcz.pl, grzegorz.biernat@im.pcz.pl
[2] *Faculty of Mathematics and Computer Science, University of Lodz, Lodz, Poland*
magdalena_wozniakowska@wp.pl

We consider the rare polynomial mappings of two complex variables having one and two zero at infinity. We prove that if the Jacobian of these mappings is constant, it must be zero. The work concerns the problems related to the Keller mappings. Recall that the Keller mapping is a polynomial mapping $F: C^2 \to C^2$ satisfies the condition $\mathrm{Jac}\, F = \mathrm{const} \neq 0$. In this work, non-Keller mapping are those whose the Jacobian being constant must vanish.

I. The rare polynomial mappings having one zero at infinity

Let $f, g: \mathbf{C}^2 \to \mathbf{C}$ be the complex polynomials of degrees $2k+1$ and $2k$, consequently, and having one zero at infinity. We consider the rare mappings of the form

$$f = X^{2k+1} + \underbrace{0 + \ldots + 0}_{k-1 \text{ zeros}} + f_{k+1} + \ldots + f_1 \tag{1}$$

and

$$g = X^{2k} + \underbrace{0 + \ldots + 0}_{k-1 \text{ zeros}} + g_k + \ldots + g_1 \tag{2}$$

where $k \geq 2$ and $f_i, g_j \in \mathbf{C}[X, Y]$ are the forms indicated degrees.

Lemma 1. *If* $\mathrm{Jac}(f, g) = \mathrm{Jac}(f_1, g_1) = \mathrm{const}$ *then* $\mathrm{Jac}(f, g) = 0$.

Proof. see [1]

II. The rare polynomial mappings having two zeros at infinity

Let $f, h: \mathbb{C}^2 \to \mathbb{C}$ are the complex polynomials of degrees $4k+2$ and $4k$, consequently, and having two zeros at infinity. Assume

$$f = X^{2k+1}Y^{2k+1} + \underbrace{0+\ldots+0}_{2k-1 \text{ zeros}} + f_{2k+2} + f_{2k+1} + f_{2k} + \ldots + f_3 + f_2 + f_1 \tag{3}$$

and

$$h = X^{2k}Y^{2k} + \underbrace{0+\ldots+0}_{2k-1 \text{ zeros}} + h_{2k} + h_{2k-1} + h_{2k-2} + \ldots + h_1 \tag{4}$$

where $k \geq 2$ and $f_i, h_j \in \mathbf{C}[X, Y]$ are the forms of the indicated degrees.

Lemma 2. *If* $\mathrm{Jac}(f, g) = \mathrm{Jac}(f_1, g_1) = \mathrm{const}$, *then* $\mathrm{Jac}(f, g) = 0$.

Proof. see [2]

The above lemma suggests that, if the polynomial mapping $(f, h): \mathbb{C}^2 \to \mathbb{C}^2$ has two zeros at infinity and the constant Jacobian, then $\mathrm{Jac}(f, h) = 0$. Therefore it remains to analyze only the case when the mapping (*f*, *h*) has only one zero at infinity, and thus takes the form

$$f = X^p + f_{p-1} + f_{p-2} + \ldots + f_1 \tag{5}$$

and

$$h = X^q + h_{q-1} + h_{q-2} + \ldots + h_1 \tag{6}$$

where f_i, h_j are the forms (of two variables) of degrees *i*, *j* respectively.

We show that there are non-trivial class of mappings having one zero at infinity with the constant Jacobian, for which that Jacobian vanish. It appears, therefore, that in the general case, the polynomial mapping having one zero at infinity and the constant Jacobian, must be vanish Jacobian. This would mean that the Jacobian conjecture takes place only in the simplest case, when

$$f = P(X) - cY \quad \text{and} \quad h = X \tag{7}$$

where $P(X)$ is a polynomial of variable *X*.

Keywords: **Jacobian, zero at infinity, rare mappings, Keller mappings**

References

[1] Pawlak E., Lara-Dziembek S., Biernat G., Woźniakowska M., An example of non-Keller maping, Scientific Research of the Institute of Mathematics and Computer Science 15(1), 115-121, 2016.

[2] Lara-Dziembek S., Biernat G., Pawlak E., Woźniakowska M., A second example of non-Keller mapping, Scientific Research of the Institute of Mathematics and Computer Science 15(2), 2016.

ON A GEOMETRY OF SOUND

Antoni Pierzchalski

Faculty of Mathematics and Computer Science, University of Lodz,
Łódź, Poland
antoni@math.uni.lodz.pl

The geometric structure of a plane domain or, more general, contained in hypersurface embedded in the Euclidean space or, even more general, on a manifold can impact the behavior of some analytic objects defined on such domains. In particular it can determine spectral properties of differential operators. It is known that selfadjoint elliptic operators on compact Riemannian manifolds have a discrete spectrum. Such spectrum can be ordered into a monotonic sequence of eigenvalues. Roughly speaking: *the geometry determines the spectrum.* In the case of the classical laplasjan this can be expressed as follows. The spectra of the Laplace operator for two isometrically congruent Riemannian manifolds coincide. We say namely that two such manifolds are isometrically congruent, if there is an isometry, i.e. a transformation of the one onto the other, preserving the metric. A question (problem) is, if the dependence take place also for other elliptic operators and what is a quantitative influence on the considered spectra. That is the essence of the so called *straight problem*. The *inverse problem* can be formulated as follows. Does, and if yes, how much, the spectrum of the Laplace or other elliptic operators determines the geometry of the domain (manifold)?

This two problems are the pivots of *spectral geometry* - a branch of mathematics that developed and braided with other branches like: differential geometry, PDEs, representations and so on. Deriving from them it was giving them at the same time a creative inspiration.

The sources of spectral geometry must be found in papers by Herman Weyl from the beginning of the past century. The ideas embodied there enlightened the whole century and constituted an inspiration to many mathematicians and also intermediately (though the Ahlfors papers) to me. Here I would like to mention two papers by Weyl [7 and 8]. They contain a spectral resolution for the Laplace operator in a domain of R^2, or the elasticity operator

$$a \text{ grad div} - b \text{ curl curl}, \qquad 3a > 4b > 0, \tag{1}$$

in a domain of R^3, where curl is the rotation of a vector field.

The Weyl formulas obtained there for thee asymptotic distribution of eigenvalues imply in particular, that the spectrum determines uniquely the volume of the domain. Let us notice by the way that both the Laplacian and the elasticity operator are elliptic.

The problems, methods and spectacular solutions attracted the attention of many mathematicians Several excellent papers have appeared. A comprehensive list of references can be found in the very good book by P. B. Gilkey [2]. To the most famous papers of the spectral geometry belongs surely the one-page paper by J. Milnor [5].

A turbulent development of the theory in the second half of the 20-th century was surely caused by the famous paper by M.Kac [4] under provocative tittle *Can one hear the shape of a drum.* This should explain, at least partially, the tittle of this exposition.

In the talk I would like to refer to problems presented in the paper [4] and with help of simple examples bring them closer to the listeners.

By the way I would like to mention also my small contribution to the subject. i.e. the paper [6] with B. Orsted. We derived there among other formulas for the asymptotic distribution of the eigenvalues of the Ahlfors operator, being on an arbitrary Riemannian manifold a counterpart of the elasticity operator (1). The formulas obtained by us reduce in the three-dimensional flat case to that of Weyl from the year 1915.

I would like to mention also some recent results by C. Gordon, B. Webb and S. Wolpert [2] or S. Zeltdich [9].

Keywords: **spectral geometry, isospectral problem, elliptic operators, ellipticity at the boundary**

References

[1] Ahlfors L.V., Quasiconformal deformations and mappings in R^n, J. Analyse Math. 30 (1976), 74–97.
[2] Gilkey P.B., Invariance theory, the heat equation and the Atiyah-Singer index theorem, Publish or Perish, Wilmington, Delaware, 1984.
[3] Gordon C., Webb D, Wolpert S., Isospectral plane domains and surfaces via Riemannian orbifolds, Invent. Math. 110 (1992), 1-22.
[4] Kac M., Can one hear the shape of a drum, Amer. Math. Monthly 73 (1966), 1–23.
[5] Milnor J., Eigenvalues of the Laplace operator on certain manifolds, Proceedings of the National Academy of Sciences of the USA 51 (1964), 542.
[6] Ørsted B., Pierzchalski A., The Ahlfors Laplacian on a Riemannian manifold with boundary, Michigan Math. J. 43 (1996), 99–122.
[7] Weyl H., Das asymptotische Verteilungsgesetz linearer partiellen Differetialglechungen, Math. Ann. 71 (1912), 441–479
[8] Weyl H., Das asymptotische Verteilungsgesetz der Eigenschwingungen eines beliebig gestalten, elastischen K¨orpers, Rendiconti di Circolo Mat. di Palermo 39 (1915), 1–49.
[9] Zelditch S, Inverse spectral problem for analytic domains, Ann. Of Math., 170, (2009), 205-269.

THE DIRICHLET PROBLEM FOR THE ONE – DIMENSIONAL TIME – FRACTIONAL ADVECTION – DIFFUSION EQUATION

Yuriy Povstenko [1], ***Joanna Klekot*** [2]

[1]*Institute of Mathematics and Computer Science, Jan Długosz University in Częstochowa, Częstochowa, Poland*
[2]*Institute of Mathematics, Częstochowa University of Technology, Częstochowa, Poland*
[1]*j.povstenko@ajd.czest.pl*, [2]*joanna.klekot@im.pcz.pl*

In the last few decades, fractional calculus has many applications in different areas of physics, geology, engineering and bioengineering [1 – 5].

In this paper the one – dimensional time fractional advection diffusion equation in a half – space is considered

$$\frac{\partial^\alpha T(x,t)}{\partial t^\alpha} = a\frac{\partial^2 T(x,t)}{\partial x^2} - v\frac{\partial T(x,t)}{\partial x} \tag{1}$$

where α denotes fractional order of Caputo derivative [6] and $0<\alpha\le 1$, $0<x<\infty$, $0<t<\infty$, $a>0, v>0$.

The equation (1) is supplemented by the zero initial condition

$$T(x,0)=0, \tag{2}$$

the zero condition at infinity

$$\lim_{x\to\infty} T(x,t)=0 \tag{3}$$

and the Dirichlet boundary condition

$$T(0,t)=g_0\,\delta(t) \tag{4}$$

with $\delta(t)$ being the Dirac delta function.

To solve the Dirichlet problem under consideration the new sought – for function is introduced

$$T(x,t)=\exp\left(\frac{v\,x}{2\,a}\right)u(x,t) \tag{5}$$

Using the Fourier sine transform with respect to the spatial coordinate x and the Laplace transform with respect to the time t gives

$$\tilde{u}^{*}(\xi,x)=a\,g_0\,\frac{\xi}{s^{\alpha}+a\,\xi^{2}+\dfrac{v^{2}}{4\,a}}\,. \tag{6}$$

Inversion of the integral transforms results in the solution

$$u(x,t)=\frac{2\,a\,g_0}{\pi}\,t^{\alpha-1}\int_0^{\infty}E_{\alpha,\alpha}\left[-\left(a\xi^{2}+\frac{v^{2}}{4\,a}\right)t^{\alpha}\right]\xi\sin(\xi\,x)\,\mathrm{d}\xi\,, \tag{7}$$

where $E_{\alpha,\beta}(\bullet)$ is the Mittag – Leffler function in two parameters α,β.

Taking into account formula (7) the equation (5) can be written in the form

$$T(x,t)=\frac{2\,a\,g_0}{\pi}\exp\left(\frac{v\,x}{2\,a}\right)t^{\alpha-1}\int_0^{\infty}E_{\alpha,\alpha}\left[-\left(a\xi^{2}+\frac{v^{2}}{4\,a}\right)t^{\alpha}\right]\xi\sin(\xi\,x)\,\mathrm{d}\xi\,. \tag{8}$$

The numerical calculations carried out using the nondimensional quantities. It is seen from the examples that decreasing of the order of the fractional derivative α leads to retardation of the mass transport process.

Keywords: **advection – diffusion equation**, **Caputo fractional derivative, Laplace integral transform, Fourier sine transform, Mittag – Leffler function**

References

[1] Metzler R., Klafter J., The random walk's guide to anomalous diffusion: a fractional dynamics approach, Physics Reports, vol. 339, 2000, 1, 1 – 77.
[2] West B. J., Bologna M., Grigolini P., Physics of Fractals Operators, Springer, New York, NY, USA 2003.
[3] Magin R., L., Fractional Calculus in Bioengineering, Begell House Publishers, Inc., Redding, CA, USA 2006.
[4] Uchaikin V. V., Fractional Derivatives for Physicists and Engineers, Springer, Berlin, Germany 2013.
[5] Povstenko Y., Fractional Thermoelasticity, Springer, New York, NY, USA 2015.
[6] Kilbas A., Srivastava H., Trujillo J., Theory and Applications of Fractional Differential Equations, Elsevier, Amsterdam 2006.

APPROXIMATE SOLUTIONS FOR STATIC PROBLEMS OF DEEP-PROFILED SANDWICH PANELS

Jolanta Pozorska [1]***, Zbigniew Pozorski*** [2]***, Łukasz Janik*** [2]

[1]*Institute of Mathematics, Czestochowa University of Technology, Czestochowa, Poland*
[2]*Institute of Structural Engineering, Poznan University of Technology, Poznan, Poland*
[1]*jolanta.pozorska@im.pcz.pl,* [2]*zbigniew.pozorski@put.poznan.pl*

Sandwich panels are typically composed of three layers: two external, thin and relatively rigid facings and a thick, but light and flexible core. From the point of view of static analysis, panels with thin and flat facings and panels with thick or deep-profiled facings are distinguished [1]. In the latter case, the structural behavior of a sandwich beam can be described by two differential equations

$$-\frac{B_D}{G_C A_C}\cdot w^{IV}+\frac{B_S+B_D}{B_S}\cdot w''=-\frac{M}{B_S}-\frac{q}{G_C A_C}-\theta\,, \tag{1}$$

$$-\frac{B_D}{G_C A_C}\cdot \gamma''+\frac{B_S+B_D}{B_S}\cdot \gamma=\frac{V}{G_C A_C}-\frac{B_D}{G_C A_C}\cdot \theta'\,, \tag{2}$$

where vertical deflection w and shear strain γ are the functions of the position coordinate x. The G_C and A_C denote shear modulus and cross-sectional area of the core, q is the distributed transverse load and θ is an initial curvature induced by a temperature difference between facings. The term B_S corresponds to the bending stiffness of the facings with respect to the global centre line of the sandwich panel, whereas B_D represents the sum of the bending stiffnesses of the facings with respect to their own centre lines. The terms M and V denote the bending moment and shear force, respectively. Deep-profiled sandwich beams are very interesting because they are internally statically indeterminate [2]. Even a simply-supported single-span beam requires six boundary conditions and thermal action always cause bending moments and shear forces. For this reason, it is tempting to apply approximate solutions that are easier to use [3, 4].

To find an approximate solution, it is assumed that the applied load is shared between two separate load-carrying systems, namely the sandwich part, which includes the influence of core shear, and the flange part which merely involves bending of the facings. These two systems are quite independent except that their deflections coincide at some critical point, usually at mid-span. In the case of a simply-supported beam carrying a uniformly distributed load q, the deflections at mid-span of the two parts (sandwich and flange) can be presented as:

$$w_S = \frac{5}{384}\frac{q_S L^4}{B_S}(1+k), \tag{3}$$

$$w_D = \frac{5}{384}\frac{q_D L^4}{B_D}, \tag{4}$$

where q_S, q_D, L and k denote the load component carried by the sandwich part, the load component carried by the flange part, the span of the beam and the shear factor, respectively. Using $q_S+q_D=q$ and $w_S=w_D$ we come to:

$$k = \frac{9.6\,B_S}{G_C A_C L^2}, \tag{5}$$

$$\delta = \frac{(1+k)B_D}{B_S + (1+k)B_D}, \tag{6}$$

$$q_S = q(1-\delta), \tag{7}$$

$$q_D = q\delta\,. \tag{8}$$

Comparing the approximate solution specified by (3-8) with the analytical solution resulting from (1-2) it can be observed that the differences between the solutions depend largely on the span of the beam. The shorter beam the greater the differences (for the span $L = 2.50$ m the relative error for the extreme displacement is 0.63%, and for $L = 5.00$ m only 0.10%). The biggest difference is for bending moment M_D (6.2% for $L = 2.50$ m). The presented approximate method, although effective, can be used only for simple static systems.

Keywords: **applied mathematics, sandwich panels, static analysis, approximations**

References

[1] Stamm K., Witte H., Sandwichkonstruktionen. Berechnung, Fertigung, Ausführung (in German), Springer-Verlag, Wien, Austria, 1974.
[2] Błaszczuk J., Pozorski Z., Engineering aspects of the mathematical model of deep-profiled sandwich panel, Scientific Research of the Institute of Math. and Comp. Sci. 2011, 2, 10, 31-42.
[3] Davis J. M., Lightweight sandwich construction, Blackwell Science Ltd., 2001.
[4] Berner K., Practical design checks for sandwich panels at the ultimate and serviceability limit states, Stahlbau, 1998, 67, 12, 910-925.

ON A CERTAIN CHARACTERIZATION OF A HOMOGENEOUS YOUNG MEASURES

Piotr Puchała

Institute of Mathematics, Czestochowa University of Technology,
Czestochowa, Poland
piotr.puchala@im.pcz.pl

Young measures appear in many engineering problems. In nonlinear elasticity, for example, we minimize the energy functional of the form

$$J(v) = \int_{\Omega} f\big(x, v(x), \nabla v(x)\big)\, dx, \tag{1}$$

where:

- Ω is elastic body under consideration;
- v is its displacement; it is usually an element of a suitable Sobolev space V;
- f is the density of the internal energy.

The so called direct method is a widely used method of minimizing such functionals.

However, energy functionals of certain materials, as laminates or various types of alloys, do not attain their infima. It is connected with what engineers call 'microstructure' and is caused by the fact, that the density of the internal energy is not quasiconvex with respect to the third variable. The minimizing sequences (v_n) are functions of a highly oscillatory nature and are divergent in the strong topology of V, but they are weakly convergent. It has been discovered by Laurence Chisolm Young in [4], that the weak* limits of the sequences of the form $\Big(f\big(x, v_n(x), \nabla v_n(x)\big)\Big)$ are in general measures, nowadays called the Young measures. The Young measure associated with a sequence is in fact a family of probability measures depending measurably on points of Ω. Its existence relies on the Riesz representation theorem. However, calculating an explicit form of a Young measure is in general a very difficult task.

The simplest form of a Young measure is a 'homogeneous Young measure'. It is in fact a 'one parameter family', i.e. it does not depend on points of Ω. It serves as a source of examples and in many real world cases it is the generalized minimizer of the considered integral functional, see for example [1] and [3].

In [2] a relatively simple method of deriving an explicit form of a homogeneous Young measure is proposed. It avoids using complicated functional analytic machinery. Instead, a change of variable theorem in multiple integrals is used.

The results presented here can be considered as a natural continuation of those in [2]. Namely, we recognize homogeneous Young measures as a certain class of

constant measure valued mappings. Then we prove an elementary characterization principle: it turns out, that the homogeneous Young measures are image measures of the Lebesgue measure with respect to the appropriate Borel function.

Keywords: **homogeneous Young measures, minimizing sequences, nonlinear functionals**

References

[1] Müller S., Variational models for microstructure and phase transitions, in Calculus of Variations and Geometric Evolution Problems, S. Hildebrandt and M. Struwe, editors, Lecture Notes in Mathematics, Vol. 1713, Springer Verlag, Berlin, Heidelberg, Germany, 1999, 85-210.
[2] Puchała P., An elementary method of calculating an explicit form of Young measures in some special cases, Optimization 2014, vol. 63 No.9, 1419-1430.
[3] Roubíček T., Relaxation in Optimization Theory and Variational Calculus, Walter de Gruyter, Berlin, New York, 1997.
[4] Young L.C., Generalized curves and the existence of an attained absolute minimum in the calculus of variations, C. R. Soc. Sci. Lett. Varsovie, Classe III, 1937, 30, 212-234.

STABILITY ANALYSIS OF AXIALLY FUNCTIONALLY GRADED EULER-BERNOULLI BEAMS

Jowita Rychlewska

Institute of Mathematics, Czestochowa University of Technology,
Czestochowa, Poland
jowita.rychlewska@im.pcz.pl

The main aim of this paper is to outline a new approach to determine the critical load of buckling of axially functionally graded (FG) beams subjected to a distributed axial load. The main idea presented here is to approximate FG beams by an equivalent beam with piecewise exponentially varying material properties, geometrical properties and axial load.

Functionally graded beams are composed of two or more materials and are characterized by a continuous variance in their material properties in the preferred direction. It is well known that beams are structural elements which carry compressive load. When compressive load crosses a critical value, elastic beam deviates from an original equilibrium state and buckling occurs. A list of papers on buckling aspects of the homogeneous structures is very extensive. For example Kukla and Skalmierski [1] presented the solution to the problem of vibrations of an Euler-Bernoulli beam, which is loaded by an axial force varying along the length of the beam. Exact mathematical solutions for buckling of structural members for various cases of beams, arches, rings, plates and shells are shown in Wang et al. [2].

The gradient variation in functionally graded beams may be oriented along the cross-section and/or axial direction. A list of papers on buckling behaviour of FG beams with thickness-wise gradient variation is very wide. For example, in paper [3] by Vo et al. the finite element model for vibration and buckling of functionally graded sandwich beams, based on a refined shear deformation theory, is presented. Li and Batra [4] derived analytical relations between the critical buckling load of a functionally graded Timoshenko beam and that of the corresponding homogeneous Euler-Bernoulli beam subjected to axial compressive load. Free vibrations, buckling and post-buckling of functionally graded beams containing open cracks, by assuming an exponential variation of material properties in the thickness direction, were studied by Yang and Chen [5].

For axially graded beams stability problems are becoming more complicated because of the governing equation with variable coefficients. For example Singh and Li [6] investigated the stability of axially functionally graded tapered beams through discretising a non-uniform column into a stepped multi-uniform column and solving a transcendental equation to compute the critical buckling load. Free vibrations and stability of axially functionally graded tapered Euler-Bernoulli beams were studied by Shahba and Rajasekaran [7] by using the differential transform element method. The finite element approach to the free vibration and

stability analysis of axially functionally graded tapered Timoshenko beams was applied by Shahba et al. [8]. A new approach to exactly calculate the critical buckling loads of beams with arbitrarily axial inhomogeneity was presented by Huang and Luo in [9].

In this study the stability analysis of axially graded beams with a distributed axial load is made. Considerations are carried out in the framework of the Euler-Bernoulli beam theory. The proposed approach is based on these presented by Kukla and Rychlewska in [10] and Rychlewska in [11]. It is assumed that the changes of material properties as well as the axial load are approximated by an exponential form. The obtained solutions of the buckling analysis for clamped-clamped, pinned-pinned, clamped-pinned and pinned-clamped beams are applied for numerical computations. Critical buckling loads are determined from the existence condition of a non-trivial solution in the resulting system of algebraic equations.

Keywords: **functionally graded beams, buckling load, Euler-Bernoulli beam theory**

References

[1] Kukla S., Skalmierski B., The effect of axial loads on transverse vibrations of an Euler-Bernoulli beam, J. Theor. Appl. Mech. 1993, 31(2), 413-430.
[2] Wang C.M., Wang C.Y., Reddy J.N., Exact Solutions for Buckling of Structural Members, CRC Press, LLC, Florida 2005.
[3] Vo T. P., Thai H-T., Nguyen T-K., Maheri A., Lee J., Finite element model for vibration and buckling of functionally graded sandwich beams based on a refined shear deformation theory, Engineering Structures 2014, 64, 12-22.
[4] Li S-R., Batra R. C., Relations between buckling loads of functionally graded Timoshenko and homogeneous Euler-Bernoulli beams, Composite Structures 2013, 95, 5-9.
[5] Yang J., Chen Y., Free vibration and buckling analyses of functionally graded beams with edge cracks, Composite Structures 2008, 83, 48-60.
[6] Singh K. V., Li G., Buckling of functionally graded and elastically restrained non-uniform columns, Composites B 2009, 40, 393-403.
[7] Shahba A, Rajasekaran S., Free vibration and stability of tapered Euler-Bernoulli beams made of axially functionally graded materials, Appl. Math. Model. 2012, 36, 3094-3111.
[8] Shahba A., Attarnejad R., Tavanaie Marvi M., Hajilar S., Free vibration and stability analysis of axially functionally graded tapered Timoshenko beams with classical and non-classical boundary conditions, Composites B 2011, 42, 801-808.
[9] Huang Y., Luo Q. Z., A simple method to determine the critical buckling loads for axially inhomogeneous beams with elastic restraint, Comput. Math. Appl. 2011, 61, 2510-2517.
[10] Kukla S., Rychlewska J., Free vibration of axially functionally graded Euler-Bernoulli beams, Journal of Applied Mathematics and Computational Mechanics, 2014, 13(1), 39-44.
[11] Rychlewska J., Buckling analysis of axially functionally graded beams, Journal of Applied Mathematics and Computational Mechanics 2014, 13(4), 103-108.

FREE AND FORCED VIBRATIONS OF COMPOSITE MEMBRANES IN POLAR COORDINATES

Urszula Siedlecka, Izabela Zamorska, Stanisław Kukla

Institute of Mathematics, Czestochowa University of Technology, Czestochowa, Poland
urszula.siedlecka@im.pcz.pl, izabela.zamorska@im.pcz.pl, stanislaw.kukla@im.pcz.pl

We consider two cases of a vibration problem: free and forced vibrations of annular and circular composite membrane . The thickness and the material density of the membrane (Fig.1) change step-wise at circles with radii $r_1, r_2, \ldots, r_{m-1}$.

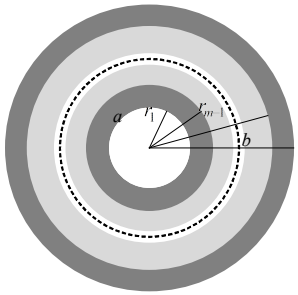

Fig. 1. A schema of the composite annular membrane.

The differential equation to vibration of a membrane is:

$$\nabla^2 u_j - \mu_j^2 \frac{\partial^2 u_j}{\partial t^2} = F(r,\theta,t), \qquad j = 1,2,\ldots,m \tag{1}$$

where $\mu_j^2 = \rho_j h_j / s$, $F(r,\theta,t) = 0$ for free and $F(r,\theta,t) = f(r,\theta,t)/s$ for forced vibrations. The functions u_j satisfy the continuity and the boundary conditions:

$$u_j(r_j,\theta,t) = u_{j+1}(r_j,\theta,t), \qquad \left.\frac{\partial u_j(r,\theta,t)}{\partial r}\right|_{r=r_j} = \left.\frac{\partial u_{j+1}(r,\theta,t)}{\partial r}\right|_{r=r_j} \tag{2}$$

$$u_1(r_0,\theta,t) = 0, \qquad u_m(r_m,\theta,t) = 0 \tag{3}$$

Additionally, for the problem of forced vibrations, the initial conditions are assumed.

Considering the free vibration of a circular membrane, we seek [1] the mode shapes in the form:

$$U_{jkn}(r) = C_{1j} J_0\left(r\omega_{kn}\sqrt{\rho_j h_j / s}\right) + C_{2j} Y_0\left(r\omega_{kn}\sqrt{\rho_j h_j / s}\right) \tag{4}$$

where the eigenfrequencies ω_{kn} are roots of equation which is obtained by using conditions (2-3):

$$\det\left(\mathbf{A}(\omega)\right) = 0 \tag{5}$$

In the case of forced vibrations, a solution to the problem we seek in the form

$$u_j(r,\theta,t) = \sum_{n=0}^{\infty}\sum_{k=1}^{\infty} U_{jkn}(r)\Gamma_{kn}(t)\cos n\theta \tag{6}$$

Substituting (6) into (1) and using the orthogonality of functions $U_{jkn}(r)$, we obtain an differential equation for the functions $\Gamma_{kn}(t)$ which is complemented by initial conditions. The solution is as follows:

$$\begin{aligned}\Gamma_{kn}(t) = {} & \frac{\cos\omega_{kn}t}{\kappa_n N_{kn}} \sum_{j=1}^{m} \mu_j^2 \int_0^{2\pi}\int_{r_{j-1}}^{r_j} r U_{jkn}(r)\, p_j(r,\theta)\cos n\theta\, dr d\theta \\ & + \frac{\sin\omega_{kn}t}{\kappa_n N_{kn}\omega_{kn}} \sum_{j=1}^{m} \mu_j^2 \int_0^{2\pi}\int_{r_{j-1}}^{r_j} r U_{jkn}(r)\, q_j(r,\theta)\cos n\theta\, dr d\theta \\ & - \frac{1}{s\kappa_n N_{kn}\omega_{kn}} \sum_{j=1}^{m} \int_0^{2\pi}\int_{r_{j-1}}^{r_j}\int_0^{t} r U_{jkn}(r)\, f_j(r,\theta,\tau)\sin\omega_k(t-\tau)\cos n\theta\, d\tau\, dr d\theta\end{aligned} \tag{7}$$

The analytical solutions of the problems, have been used to perform numerical computations [1-2] to show the effects of parameters characterized the non-uniformity of composite membranes on the vibrations.

Keywords: **composite membrane, free vibrations, forced vibrations**

References

[1] Siedlecka U., Zamorska I., Kukla S., Vibration analysis of composite circular and annular membranes, Journal of Applied Mathematics and Computational Mechanics, 2016, 15(1), 149-159.

[2] Jabareen M., Eisenberger M., Free vibrations of non-homogeneous circular and annular membranes. Journal of Sound and Vibration, 2001, 240(3), 409-429.

STABILITY OF THE NON - PRISMATIC COLUMN UNDER THE GENERALISED LOAD BY A FORCE DIRECTED TOWARDS THE POSITIVE POLE

Janusz Szmidla, Anna Jurczyńska

Institute of Mechanics and Machine Design Foundations, Czestochowa University of Technology, Czestochowa, Poland
j.szmidla@imipkm.pcz.pl, a.jurczynska@imipkm.pcz.pl

The results of the theoretical and numerical studies concerning the issue of the stability of the slender non-prismatic column [1] subjected to the generalised load by a force directed towards the positive pole (the case of the specific load [2]) are presented in this work. Changeability of the cross-section of the considered system along its axis was modelled due to column dividing into the n smaller prismatic segments of constant length l and thickness h and variable width b. In this studies it was assumed that the total volume of each segment is constant. Additionally, the width b of the particular element should be greater than or equal to the thickness h ($b \geq h$). An approximation of the shape of the column by the linear function $b(x) = 2 \cdot a(Z) \cdot x + d$ and by the polynomial of degree 2 $b(x) = 2 \cdot \left[a(p,q) \cdot [x - p]^2 + q\right]$, where $x \in \langle 0; L \rangle$ was analysed in this work. The considered case of the specific load is realised by the loading and receiving heads, built of the elements of circular outlines [3] (constant curvature).

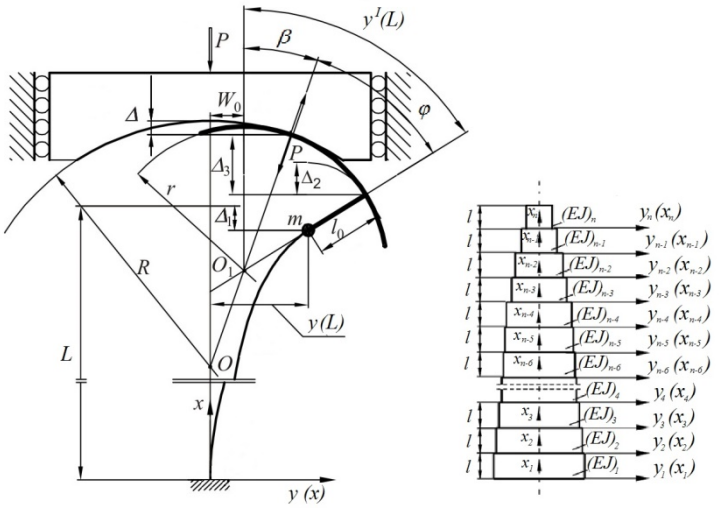

Fig. 1. The physical model of the considered nonprismatic column

On the basis of the defined physical model, taking into account Bernoulli - Euler's theory, the total potential energy of the system was determined. Based on the static criterion of the loss of the stability (the principle of the minimum potential energy) [4], the boundary problem was formulated. The differential equations of the transverse displacements and the geometrical and natural boundary conditions were defined.

By substituting obtained solutions of the differential equations of the displacements into the boundary conditions and the continuity conditions, the value of the critical load of the analysed column was determined. The performance of series of numerical computations allowed to the designation of the influence of the shape of the considered system and the geometrical parameters of the structure implementing external load on the stability of the nonprismatic column. For the boundary problem, as defined above, looking for shapes that are the most advantageous leads up to the selection of the appropriate values of the width of the cross-section of the each segments in such a way that the transferred critical force is a s large as possible (calculation of the global maximum of the function of the critical load).

Keywords: **stability, non-prismatic systems, specific load**

References

[1] Szmidla J., Kluba M., Stateczność i drgania swobodne niepryzmatycznego układu smukłego poddanego obciążeniu eulerowskiemu, Modelowanie Inżynierskie, 2011, 41, 385-394.
[2] Tomski L., Obciążenia układów oraz układy swoiste, L. Tomski [red], Drgania swobodne i statecznośc obiektów smukłych jako układów liniowych lub nieliniowych, Wydawnictwo Naukowo- Techniczne, Fundacja Książka Naukowo-Techniczna, Warszawa 2007, 17-46.
[3] Kasprzycki A., Opis techniczny struktur obciążających kolumny, L. Tomski [red], Drgania swobodne I statecznośc obiektów smukłych jako układów liniowych lub nieliniowych, Wydawnictwo Naukowo-Techniczne, Fundacja Książka Naukowo-Techniczna, Warszawa 2007, 47-60.
[4] Tomski L., Szmidla J., Wprowadzenie do problematyki stateczności I drgań swobodnych kolumn, L. Tomski [red], Drgania i stateczność układów smukłych, Wydawnictwo Naukowo- Techniczne, Fundacja Książka Naukowo-Techniczna, Warszawa 2004, 15-39.

STABILITY OF THE NON - PRISMATIC COLUMN SUBJECTED TO THE SELECTED CASE OF THE SPECIFIC LOAD REGARDING THE JOINT FLEXIBILITY

Janusz Szmidla, Anna Jurczyńska

Institute of Mechanics and Machines Design Foundations, Czestochowa University of Technology, Czestochowa, Poland
j.szmidla@imipkm.pcz.pl, a.jurczynska@imipkm.pcz.pl

Theoretical considerations and results of numerical simulations relating to the issue of the stability of a slender nonprismatic column subjected to the selected case of a specific load are presented in this work. Carried out studies included the flexibility of structural joints of the mounting and the structure implementing load [1].

Geometry of the column analysed in this paper is presented in figure 1. Modelling of a cross-section variable along the axis was possible to achieve thanks to dividing the column into n smaller segments of constant thickness h and length l where $l \cdot n = L = const.$. According to the assumed extra condition of constant total volume of the system $V_{obj} = const.$, variable along the axis width of the cross-section b was described by means of linear function $b(x) = 2 \cdot a(Z) \cdot x + d$ and polynomial of degree 2 $b(x) = 2 \cdot \left[a(p,q) \cdot [x - p]^2 + q\right]$, where $x \in \langle 0; L \rangle$. Load by a follower force directed towards the positive pole (the case of specific load) is guaranteed by the elements of circular outlines - loading and receiving heads [2]. Load is transferred to the column by the rigid element of length l_0. Force P is tangential to the deflection of free end of the system and its directions passes through the stationary point O located on the undeformed axis of the column below the free end of the system (the positive pole). In the physical model of the column, the flexibility of structural joints in the mounting (elasticity C_1, $x = 0$) and in a support of the free end (springs of the elasticity C_2 and C_3, $x = L$) was taken into consideration.

On the basis of the physical model of the analysed column the mathematical model of the system was defined. The total potential energy was determined. Based on a static criterion of stability loss, after prior calculations of the potential energy variation, the differential equations of displacement and the natural boundary conditions were obtained. The development of the calculations programmes allowed for the multidimensional analysis of the issue of the stability of considered column.

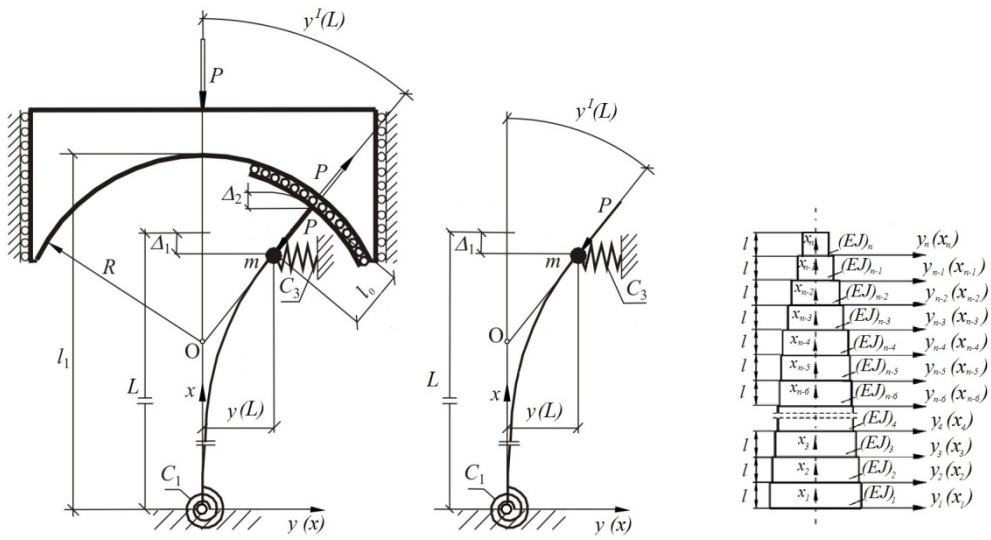

Fig. 1. The physical model of nonprismatic system subjected to the follower force directed towards the positive pole regarding to the flexible of the structural joints [1, 3]

The results of numerical calculations determining the influence of the variable cross-section of the column along the axis of the system, the elasticity of the flexible structural joints and the geometry of structure implementing the external load on the value of the transferred critical force were included in this work. The results were presented in the dimensionless form and referred to the appropriate values obtained in the case of a prismatic system of the same total volume, which is a comparative system. Taking into account assumed scope of the width of the cross-section, the most advantageous shapes of the considered nonprismatic system, for which the obtained increases in the critical load were the biggest, were indicated.

Keywords: **non-prismatic systems, stability, specific load, joint flexibility**

References

[1] Tomski L., Podgórska-Brzdękiewicz I., Dragania swobodne I stateczność kolumn poddanych obciążeniu swoistemu- podatne węzły konstrukcyjneukładu wymuszającego I przejmującego obciążenie, L. Tomski [red], Drgania I statecznośc układów smukłych, Wydawnictwo Naukowo-Techniczne, Fundacja Książka Naukowo-Techniczna, Warszawa 2004, 134-187.

[2] Kasprzycki A., Opis techniczny struktur obciążających kolumny, L. Tomski [red], Drgania swobodne I statecznośc obiektów smukłych jako układów liniowych lub nieliniowych, Wydawnictwo Naukowo- Techniczne, Fundacja Książka Naukowo-Techniczna, Warszawa 2007, 47-60.

[3] Tomski L., Obciążenia układów oraz układy swoiste, L. Tomski [red], Drgania swobodne i statecznośc obiektów smukłych jako układów liniowych lub nieliniowych, Wydawnictwo Naukowo- Techniczne, Fundacja Książka Naukowo-Techniczna, Warszawa 2007, 17-46.

VERYFICATION OF PEOPLE BASED ON PALM VEIN WITH THE ROI AUTOMATICA APPOINTMENT

Dorota Smorawa, Mariusz Kubanek

Institute of Computer and Information Sciences, Czestochowa University of Technology, Czestochowa, Poland
dorota.smorawa@icis.pcz.pl, mariusz.kubanek@icis.pcz.pl

Currently there are variety of types of biometric systems based on signature [1], gait [2], fingerprint [3], hand geometry [4] or palm print [5]. Each of these systems is to less or more extent burdened with some defects. Some biometric features can be easily prepared, for example fingerprints. The next example can be a palm print when a finger having been wounded makes the print look differently and will not be accepted by the system. The biometric system based on palm vein does not have these defects. The vein pattern is unique and unchanging for each person. This trait can be collected in a non invasive and safe way. The blood vessels pattern cannot be faked because the vessels are under the skin. The acquisition of the pattern is carried out by lighting the hand with the near- infrared light. The image is taken with a CCTV active-matrix infrared camera. Furthermore, living features are automatically checked with the systems.

Presently, in the field of hand blood vessels research a few interesting methods to create the biometric systems based on vein pattern can be found. In the papers [6] there is a description of the construction of biometric system based on palm vein, which uses a two-dimensional Gaussian function to create filters with which the image is being searched to find as many blood vessels as possible. Hamming distance was used for pattern matching. In other works [7] a three-stage algorithm was proposed allowing to create the biometric system to identify people by means of blood vessels in a hand. The contrast enhancement and thresholding of hand blood vessels belong to the first stage of the project. The feature extraction and matching are based on the Gabor wavelet. In another research work [8] Jacobi algorithm is used to find vein and characteristic points. The well-known Euclidean distance was used for pattern matching.

Defining the region of interest (ROI) is one of the most important steps in creation of the biometric system based on the hand blood vessels. Employment of the ROI allows building a biometric system and facilitates the user's authorization. One of the first steps in the proposed method is the extracting of the hand area by binarization. Then, the points P_1, P_2, P_3 are determined. These points define hand border between fingers. Through the P_1 and P_2 points the line S is placed. The parallel line L is appointed to the lower edged of the image which at the same time crosses the point P_1. The angle θ (1) between the S and L lines is used to rotate the hand with respect to the coordinate system.

$$\theta = a\tan\left(\frac{YP_2 - YP_1}{XP_2 - XP_1}\right) \tag{1}$$

The next step is connecting P_1 and P_2 points. The distance between those points defines the height and the width of the determined area.

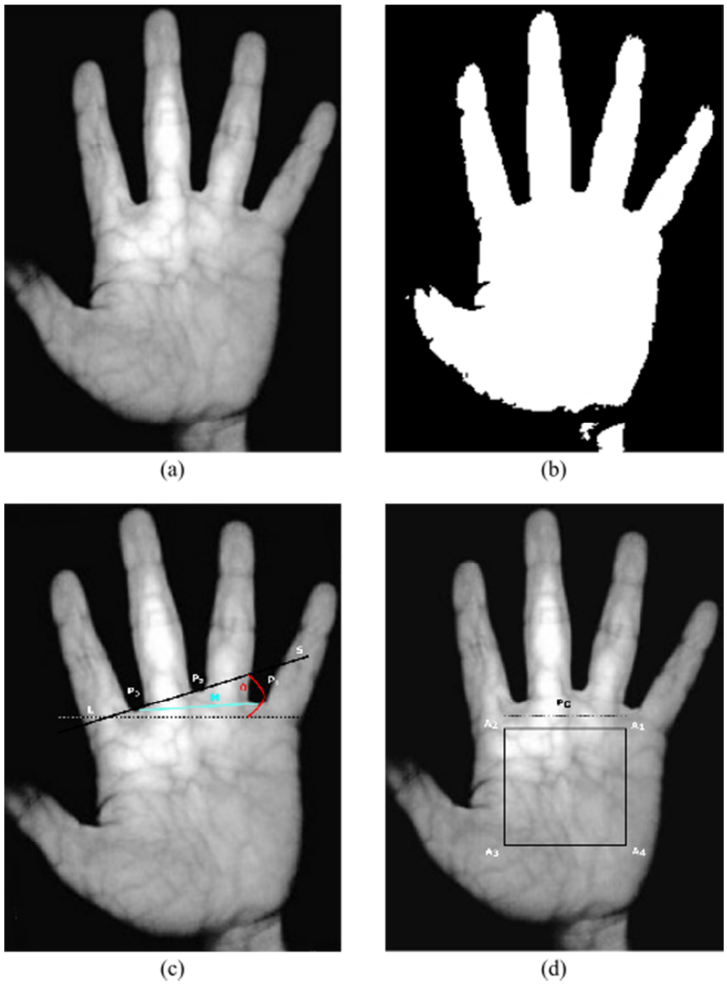

Fig.1. Palm vein image preprocessing: **a)** Original palm vein, **b)** Binary palm vein image, **c)** two data points P_3 and P_2 are selected and the palm image is rotated an angle θ between lines *S* and *L* **d)** based on line *M*, a square region is located and denoted as the ROI

To extract features a two-dimensional density function is used, described by the following formula (2):

$$f(x,y) = \frac{1}{2\prod\delta^2}\exp\left(\frac{-\left(x^2+y^2\right)}{2\delta^2}\right) \tag{2}$$

One of the steps is designing the filters to localize the curvature horizontally and vertically and two diagonally, where the first and second derivative of two-dimensional density function will be used. Based on curvatures, local maximal points along the cross-section of the input image will be determined. The next step is to connect the designated vein centres and all veins positioning. This is done basically by checking m pixels located to the right and left of (x, y) along the adopted projection direction. With so designated a vein line for all considered directions the final pattern of blood vessels is created.

To create the features vector the characteristic elements were used as it was similarly applied in the minutiae, used to analyse fingerprint, ending and bifurcation veins.

Keywords: **palm vein, ROI, biometric system, two-dimensional density function**

References

[1] Gluhchev G., Savov M., Boumbarov O., Vasileva D., A New Approach to Signature – Based Authentication, Advances in Biometrics, Lecture Notes in Computer Science, 2007, 2, 594-603.
[2] Goffredo M., Spencer N., Pearce D., Carter J. N., Nixon M. S., Human Perambulation as a Self Calibrating Biometric, Analysis and Modeling of Faces and Gestures, Lecture Notes in Computer Science, 2007, 1, 139-153.
[3] Kasban H., Fingerprints Verification Based on Their Spectrum, Neurocompiuting, 2016, 171, 910-920.
[4] Sharma S., Dubey S. R., Singh S. K., Saxena R., Singh R. K., Identity Verification Using Shape and Geometry of Human Hands, Expert Systems With Applications, 2015, 2, 821-832.
[5] Zheng P., Gaussian Shape Descriptor for Palmprint Authentication, Cogn Comput, 2010, 2, 303-311.
[6] Wu K-S., Lee J-C., Lo T-M., Chang K-C., Chang C-P., A Secure Palm Vein Recognition System, The Jurnal of Systems and Software, 2013, 86, 2870-2876.
[7] Wang R., Wang G., Chen Z., Zeng Z., Wang Y., A Palm Vein Identification System Based on Gabor Wavelet Features, Neural Comput & Applic, 2014, 24, 161-168.
[8] Sonal S-A., Dhiraj P., Pallavi D., Yogesh H-D., Hardware Implementation of Palm Vein Biometric Modality for Access Control in Multilayered Security System, Procedia Computer Science, 2015, 58, 492-498.

INFLUENCE OF THE PARAMETERS OF THE LOADING HEADS ON FREE VIBRATIONS OF THE CRACKED COLUMN

Krzysztof Sokół, Sebastian Uzny

Institute of Mechanics and Machine Design Foundation, Czestochowa University of Technology, Czestochowa, Poland
sokol@imipkm.pcz.pl, uzny@ imipkm.pcz.pl

The considered in this study external load was introduced into scientific literature by L. Tomski [1]. The specific load is realized by means of the loading heads with the outlines in the shape of circular, parabolic or linear elements. The load can be realized by: generalized load with a force directed towards a negative or positive pole or a follower force directed towards a negative or positive pole - point localized below the loaded end of the column on its undeformed axis. The line that connects the pole and the loaded end of the structure creates a line of action of external load.

In the figure 1 the investigated column is presented. The damage of the system is in the form of one sided open crack which is simulated by means of the rotational spring of stiffness C. Furthermore the crack divides a slender structure into two elements. The element length relation is as follows – total length $l = l_1+l_2$. In the point of the crack presence the continuity of transversal and longitudinal displacements as well as bending moments and deflection angles are satisfied by natural boundary conditions. The external load marked as P is realized by the loading heads with circular outlines. On the loaded end the mass m is placed in order to simulate the mass of the loading heads.

The loading structure is composed of two elements. The first one (load inducing head) has radius R. The radius R has a center in the pole to which an external force is directed. The second head (load receiving head) has radius r. The distance between the top end of the column and the contact point of heads is marked as l_0.

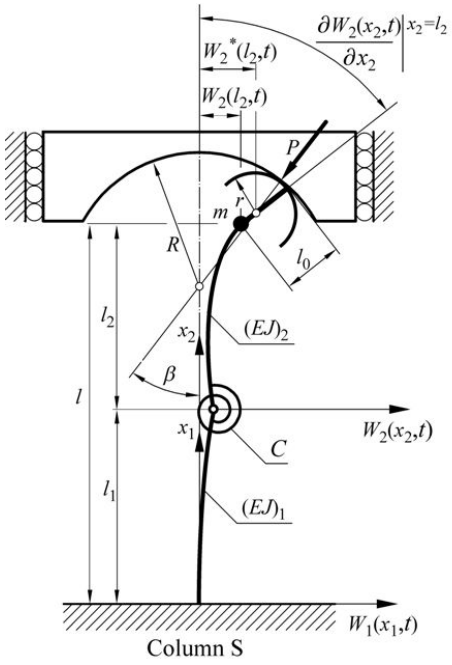

Figure 1. Investigated system subjected to generalized load by a force directed towards a positive pole

The boundary problem is formulated with the use of the Hamilton's principle in the form: $\delta\int_{t_1}^{t_2}(\mathrm{T}-V)dt=0$.

The main scope of this theoretical investigations is to present an influence of the parameters of the loading heads on instability, free vibrations and critical load magnitude of the column presented in the figure 1. Such a combination of the loading heads parameters is searched at which the column will be the least sensitive to defect presence.

Keywords: **Specific load, crack, kinetic stability criterion, column, loading head**

References

[1] Tomski L., Gołębiowska Rozanow M., Szmidla J., Free Vibration of a Column Loaded by a Force and Bending Moment, Vibrations in Physical Systems 1994, Poznań – Błażejewko, 317–319.

RELATIONSHIP BETWEEN PRIORITY RATIOS DISTURBANCES AND PRIORITY ESTIMATION ERRORS

Tomasz Starczewski

Institute of Mathematics, Czestochowa University of Technology,
Czestochowa, Poland
starczewski.t@gmail.com

This article is devoted to some problems connected with multicriteria decision analysis, wherein the *pairwise comparison matrix* (PCM) is the basic source of information about decision maker's preferences. Based on such a PCM one can estimate a *priority vector* (PV) i.e. a vector of priority weights assigned to considered decision alternatives. There are a number of prioritization methods allowing us to obtain the PV from the PCM. They work well when the PCM is consistent i.e. when it satisfies the following definitions, [7]:

Definition 1

A given matrix $\mathbf{A}=[a_{ij}]_{nxn}$ is called *reciprocal* PCM if the condition $a_{ij}=1/a_{ji}$ holds for any $i,j=1,\ldots n$.

Definition 2

A given matrix $\mathbf{A}=[a_{ij}]_{nxn}$ is called *consistent* PCM (or *cardinally* transitive) if it is reciprocal and its elements satisfy the condition: $a_{ij}a_{jk}=a_{ik}$ for all $i, j, k=1,\ldots,n$.

The necessary and sufficient condition for any positive matrix **A** to be consistent is the existence of a *certain* vector **w** satisfying $a_{ij}=w_i/w_j$ for all $i,j=1,\ldots,n$.

It is argued that good decision maker gives "consistent" judgements about priority ratios, but the real-world practice shows something different. The human brain is not a perfect calculating machine so the decision maker's judgements do not create a perfectly consistent PCM. The errors may be the result of the usage of a limited number of allowed estimates (so-called scales), human brain limitations or they may have other sources. In every case the very important question is: whether we can use a given PCM to derive the decision maker's priority vector? In order to answer this question, various *inconsistency indices* have been introduced in literature. However it is still not known whether the smaller value of a given index is related to smaller value of PV estimation errors. In our presentation we show examples that it is not always the truth. Thus another fundamental question arises: what is the relationship between priority ratios disturbances and PV estimation errors?

More precisely, following the idea presented in [4,5,6,7], we assume the following stochastic model for the judgments about priority ratios given by the decision maker in the PCM:

$$a_{ij} = \varepsilon_{ij} \frac{w_i}{w_j} \tag{1}$$

Probability distributions of the so-called perturbation factor ε_{ij} mainly involve log-normal, gamma, uniform (e.g. Budescu et al 1986, Zahedi 1986, Basak 1998, Grzybowski 2010) and truncated normal (e.g. Choo & Wedley 2004, Lin 2007, Grzybowski 2012). Apart from these most popular probability distributions, one can also find applications of the Laplace, Couchy, triangle and beta p.d., for discussion see e.g. Dijkstra 2014 .

In our paper we study the relationship between the probability distribution of the perturbation factor in (1) and the distribution of PV estimates errors. For this purpose we make use of the Monte Carlo simulations. In our studies we adopt the simulation framework introduced in [Grzybowski 2016]. Within this simulation setup we generate perfect PCM based on randomly selected "true" PV and then we disturb it assuming different distributions of ε_{ij} in (1) . Next we derive the estimate of the PV from such a PCM and analyze the estimation errors, i.e. the relative diffrence between the "true" and the estimated PV. The errors are given by the following formula:

$$\mathrm{RE}(\boldsymbol{v},\boldsymbol{w}) = \frac{1}{N}\sum_{i=1}^{N}\frac{|v_i - w_i|}{v_i}$$

Finally we calculate and compare the statistical characteristics of the above RE distributions and study their relationship with the characteristics of the perturbation factor characteristics.

Keywords: **pairwise comparisons, perturbation factor distribution, Monte Carlo, priority estimates errors, AHP**

References

[1] Budescu, D.V., Zwick R., & Rapoport A., Comparison of the analytic hierarchy process and the geometric mean procedure for ratio scaling, Applied Psychological Measurement, 10, 1986, 69-78.
[2] Dijkstra, T.K., On the extraction of weights from pairwise comparison matrices, Central European Journal of Operations Research, 21(1), 2013, 103- 123.
[3] Grzybowski A.Z., Note on a new optimization based approach for estimating priority weights and related consistency index, Expert Systems with Applications , 39, 2012, 11699–11708.
[4] Grzybowski, A.Z., New results on inconsistency indices and their relationship with the quality of priority vector estimation, Expert Systems With Applications 43, 2016, 197–212
[5] Lin, C-C., A Revised Framework for Deriving Preference Values from Pairwise Comparison Matrices, European Journal of Operational Research , 176, 2007, 1145-1150.
[6] Saaty, T.L., The Analytic Hierarchy Process, McGraw Hill, New York, 1980.

SELECTED EXAMPLES OF COALGEBRAS FOR BEHAVIOR OBSERVATION

William Steingartner, Valerie Novitzka

Faculty of Electrical Engineering and Informatics, Technical University of Košice, Košice, Slovakia
william.steingartner@tuke.sk, valerie.novitzka@tuke.sk

Abstract: In this paper we present several selected examples illustrating observing of behavior by coalgebras. We show this approach on the example of bank account, infinite lists and Fibonacci numbers.

1. INTRODUCTION

We present in this paper some motivating examples of coalgebras. After the necessary section with the basic notions we introduce some motivating examples of coalgebras. Examples are inspired by practical problems from applied computer science. We show basic formulation and construction of coalgebras on very famous practical problems – simple description of bank account and important operations over it, on Fibonacci numbers and on (possibly) infinite lists.

Coalgebras are very important part of theoretical computer science. Their main role is in describing the generated behavior of running programs [1, 2]. This is the behavior that can be observed on the outside of a machine, for instance on the screen. Coalgebra is an abstract notion of observable behavior. It is a study of states and their operations and properties. The set of states is usually seen as a black box, to which one has limited access [3]. A relation between what is actually inside and what can be observed externally is the foundation of the theory of coalgebras [2]. Coalgebras include many familiar systems, e.g. streams, trees, automata, relations etc.

2. BASIC NOTIONS

We start with the definition of F-coalgebras for endofunctor. An F-coalgebra, also called coalgebra of type F or F-system, is a pair $\langle C, c \rangle$, where C is a state space (or base set) of the coalgebra and c is the structure map of the coalgebra on C:

$$c : C \to FC.$$

This structure map acts as a destructor. It takes an element of the coalgebra and decomposes the element into its constituent parts. This is a common feature of coalgebras and this point of view is dual to the point of view that algebras are objects together with combinatory principles [4].

A coalgebra homomorphism form a commutative square (Fig. 1) and the coalgebras and their homomorphisms form a category of coalgebras. The identity map is always a homomorphism and the composition of two homomorphisms is again a homomorphism. This is an immediate consequence of the conditions defining the functor. Thus, for a given functor F, the class of all F-coalgebras forms a category [5]

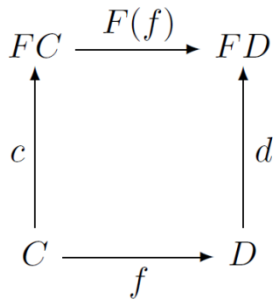

Fig. 1 Commutative diagram for coalgebras

3. EXAMPLES

We illustrate here three interesting examples of coalgebras and their application in computer science: coalgebraic description of simple bank account, infinite lists and Fibonacci numbers.

3.1 Bank account

Let X be interpreted as a collection of very rudimentary bank account states similar to [5]. At a state x of the carrier, two usual operations are possible: to show the actual balance attribute of the state, $balance(x)$ or to modify the account state to a new state $deposit(x, n)$ using an input real n. Let these functions be defined as follows:

$$balance : X \to R$$
$$deposit : X \times R \to X$$

After applying the currying on deposit, a coalgebra structure map is defined as follows:

$$c : X \to X^R \times R.$$

Taking the functions *balance* and *deposit* together, structure map is defined as $c = \langle balance, deposit \rangle$. A bank account with these functions is a coalgebra for the functor $F(X) = X^R \times R$. It holds

$$\pi_2 \circ c = balance,$$
$$(\pi_1 \circ c)(x)(n) = deposit(x, n),$$

where the maps π_1 and π_2 stand for obvious projections defined to product.

This coalgebra models a correct bank account which records in the state the history of all deposited sums and returns the total balance on the account when the function *balance* is applied.
Let the state space X be the set of finite strings over reals and let the symbol $\Sigma(x)$ denotes the sum of all reals in x. Then the functions in coalgebra are defined as follows:

$$balance(x) = \Sigma(x),$$
$$deposit(x, r) = x :: r,$$

where double colon denotes the operation join into the list (sequence).

3.2 Infinite lists as coalgebras

Viewing a data structure as being perpetually in the process of creation, rather than as a result of a completed computation is typical for observation of behavior [6]. According to this view a list may be thought of as a partial computation that, when induced, computes just far enough to determine whether the end of the list has been reached, or , if not, to produce the next element of the list together with a suspended computation to compute the remainder of the list. Then possible to define infinite lists (also known as streams) that continually generate the next element, without ever reaching the end of the list [4].

Let X be a state space. A coalgebra for lists is given by a set X and two maps

$$head : X \to A$$
$$tail : X \to X$$

where A is a fixed set of values. A structure map of coalgebra is defined as follows:

$$c : X \to A \times X,$$

Where operations *head* and *tail* are parts of structure map $c = \langle head, tail \rangle$. Now we consider the set functor

$$F(X) = A \times X$$

for a fixed set A. A coalgebra for this functor consists of a set X and a structure map

Given any such coalgebra, each value $x \in X$ gives rise to an infinite stream over the set A, namely:

$$head(x),\ (tail \circ head)(x),\ (tail^2 \circ head)(x),\ \ldots$$

Hence, for any F-coalgebra $\langle X, \varphi \rangle$, we can define a mapping f from X to the collection of (possibly infinite) streams over X (denoted X^∞), by defining

$$f(x) = \begin{cases} () & \text{if } c(x) \text{ is undefined;} \\ \lambda n.(tail^n \circ head)(x) & \text{otherwise.} \end{cases}$$

The map f is an example of coalgebra homomorphism. In the second case, the resulting function may be defined only for certain value n.

3.3 Coalgebra for Fibonacci numbers

We close this section with the well-known mathematical structure of Fibonacci numbers that are formulated coalgebraically. This example was inspired by approach in [3]. In object-oriented languages class is a structure that encapsulates data with operations on them. A coalgebraic specification can be seen as specification of such a class, where observers capture the data and the methods their operations.

Coalgebraic specification *Fibonacci*

Operations:

$val : X \to N$
$next : X \to X$

Assertions:
$val(next(next(x))) = val(next(x)) + val(x)$

Creation:
$val(new) = 1$
$val(next(new)) = 1$

Fig. 2 A coalgebraic specification of a Fibonacci numbers system

An initial state is considered as *new*. A model of a coalgebraic specification consists of a structure map of coalgebra c and of an initial state that satisfies the creation conditions. As a state space we take a set

$$X = \{(f, n) \in N^N \times N \mid \forall m \geq n.f(m + 2) = f(m + 1) + f(m)\}$$

together with the operations:

$$val(f, n) = f(n) \text{ and } next(f, n) = (f, n + 1).$$

The resulting coalgebra structure map c is $\langle val, next \rangle : X \to N \times X$ and it satisfies the assertion from coalgebra specification in Fig. 2. As an initial state we take a tuple $new = (fib, 0) \in X$, where the function $fib : N \to N$ is recursively defined Fibonacci function satisfying $fib(0) = 1$, $fib(1) = 1$ and $fib(m + 2) = fib(m + 1) + fib(m)$, for all $m \in N$. Here the states $(f, n) \in X$ implicitly keep track of the stage n in the infinite sequence of Fibonacci numbers.

4. CONCLUSION

We presented in this paper very fruitful examples of describing the behavior of several systems known from practice. These systems were considered as transition systems. Our next goal is to investigate bisimilarity, the relation between states and coinductive proofs of behavior.

Acknowledgment

This work was supported by Grant No. FEI-2015-18: Coalgebraic models of component systems.

Keywords: **coalgebra, observable behavior, category theory**

References

[1] Adámek J., Milius S., Moss L. S., Initial algebras and terminal coalgebras: a survey, 2010.
[2] Jacobs B., Rutten J., An introduction to (co)algebras and (co)induction. In: D. Sangiorgi and J. Rutten (eds), Advanced topics in bisimulation and coinduction, 2011 (This chapter is a modest update of the 1997 BEATCS old tutorial paper).
[3] Jacobs B., Introduction to Coalgebra. Towards Mathematics of States and Observations, Version 2.0, 2012.
[4] Hughes J., A study of categories of Algebras and Coalgebras, Ph.D. thesis, Carnegie Mellon University, Pittsburgh PA, 2001.
[5] Gumm P., Elements Of The General Theory Of Coalgebras, 1999.
[6] Slodičák V., Macko P., Some New Approaches in Functional Programming Using Algebras and Coalgebras. In: Electronic Notes in Theoretical Computer Science. Vol. 279, no. 3 (2011), 41-62.

MULTI-SERVER CLOSED QUEUEING SYSTEM WITH LIMITED BUFFER SPACE

Oleg Tikhonenko, Anna Tikhonenko-Kędziak

Faculty of Mathematics and Natural Sciences. College of Sciences,
Cardinal Stefan Wyszyński University in Warsaw,
Warsaw, Poland
o.tikhonenko@uksw.edu.pl, a.tikhonenko@uksw.edu.pl

Queueing systems with requests of random space requirement (or random volume) are the generalization of the classical queueing models [1, 2]. They can be used to model and solve various practical problems in design of computer and communicating systems. In particular, such models can be applied for buffer space volume determination in the nodes of communication networks.

Consider the closed system [3–5] in which N terminals are served by n identical servers. Each terminal generates its request after some thinking time having an exponential distribution with parameter λ. We assume that each request needs some memory space. The size of such need (i.e. request volume) we denote by ζ and assume that ζ is a non-negative (discrete or continuous) random value (RV).

Let $L(x) = P\{\zeta < x\}$ be the distribution function (DF) of the RV ζ. We denote by $\eta(t)$ the number and by $\sigma(t)$ the total volume of requests present in the system at time instant t. The values of process $\sigma(t)$ are limited by constant value $V > 0$ that is named memory volume of the system. Assume that the system under consideration contains the common queue with $m \le N - n$ waiting places.

We denote our system by the notation $M/M/n/m/(N,V)$.

At the epoch τ of the generation process termination, the request of volume y is accepted to the system if $\eta(\tau^-) < n + m$ and $\sigma(\tau^-) + y \le V$. Then, we have $\eta(\tau) = \eta(\tau^-) + 1$ and $\sigma(\tau) = \sigma(\tau^-) + y$. In opposite case, we have $\eta(\tau) = \eta(\tau^-)$ and $\sigma(\tau) = \sigma(\tau^-)$, the request will be lost and the terminal starts generation of the next one.

The accepted request starts its service by one of free servers, if $\eta(\tau) \le n$. In opposite case, the request waits for service in the queue. We assume that the order of requests service is in congruence with FIFO discipline. Service time doesn't depend on the request volume and has an exponential distribution with parameter μ. If the request of any terminal was accepted to the system, the generation of the next request starts after its service termination.

For the system under consideration, we determine the stationary distribution of the number of requests present in the system and the loss probability of a request.

Let η be the steady-state number of requests in the system. Introduce the notation:

$$p_k = P\{\eta = k\},\ k = 1, 2, ..., n+m.$$

We prove that

$$p_k = \begin{cases} p_0 \binom{N}{k} \rho^k L_*^{(k)}(V), & 1 \le k \le n; \\ p_0 \dfrac{N!\rho^k}{(N-n)!n!n^{k-n}} L_*^{(k)}(V), & n+1 \le k \le n+m, \end{cases}$$

where

$$p_0 = \left[\sum_{k=0}^{n} \binom{N}{k} \rho^k L_*^{(k)}(V) + \sum_{k=n+1}^{n+m} \frac{N!\rho^k}{(N-k)!n!n^{k-n}} L_*^{(k)}(V) \right]^{-1},$$

$L_*^{(k)}(V)$ is the k-fold Stieltjes convolution [6] of the DF $L(x)$ for $x = V$.

For request steady-state loss probability P_{loss} we obtain the relation:

$$P_{\text{loss}} = 1 - \frac{\sum_{k=1}^{n} k p_k + n \sum_{k=n+1}^{n+m} p_k}{\rho \sum_{k=0}^{n+m} (N-k) p_k},$$

where $\rho = \lambda / \mu$.

Keywords: **total requests capacity, memory space, loss probability, Stieltjes convolution**

References

[1] Tikhonenko O., Probability methods of information system analysis, Akademicka Oficyna Wydawnicza EXIT, Warsaw, 2006 (in Polish).
[2] Tikhonenko O.M., Queueing models in information systems, Universitrtskoe, Minsk, 1990 (in Russian).
[3] Bocharov P.P., D'Apice C., Pechinkin A.V., Salerno S., Queueing Theory, VSP, Utrecht–Boston, 2004.
[4] Gnedenko B. V., Kovalenko I. N., Introduction to Queueing Theory, Birkhäuser, Boston, 1989.
[5] Breuer L., Baum D., An Introduction to Queueing Theory and Matrix-Analytic Methods, Springer, 2005.
[6] Feller W., An Introduction to Probability Theory and its Applications, Vol. 2. Wiley, New York, 1971.

HEAT SOURCE MODELS IN ANALYTICAL DESCRIPTIONS OF TEMPERATURE FIELDS IN WELDING PROCESSES

Jerzy Winczek

Institute of Mechanical Technologies, Czestochowa University of Technology, Czestochowa, Poland
winczek@imipkm.pcz.pl

The first attempts to describe the temperature field in welding and allied processes in the middle of the last century have been undertaken. Modeling the temperature field during welding was initiated by works by Rosenthal [1] and Rykalin [2], who assumed point and linear models of heat source, respectively.

For analytical description of the temperature field the heat conduction differential equation is commonly used [3]:

$$a\nabla^2 T(\mathbf{r},t) = \frac{\partial T(\mathbf{r},t)}{\partial t} - \frac{1}{c\rho}\frac{\partial Q}{\partial t} \tag{1}$$

where **r** denotes the radius vector of the considered point in relation to the the heat source, T - temperature, t – time, a - thermal diffusivity, c – specific heat, ρ – density, Q – heat source.

In the case of a point source the solution of equation (1) for infinite body is in the form:

$$T(R,t) - T_0 = \frac{Q}{c\rho(4\pi at)^{1.5}} \exp\left(-R^2/4at\right) \tag{2}$$

R denotes the distance from the source to considered point. For semi-infinite body the solution is:

$$T(R,t) - T_0 = \frac{2Q}{c\rho(4\pi at)^{1.5}} \exp\left(-R^2/4at\right) \tag{3}$$

or

$$T(x,y,z,t) - T_0 = \frac{2Q}{c\rho(4\pi at)^{1.5}} \exp\left(-\frac{(x-x')^2 + (y-y')^2 + z^2}{4at}\right) \tag{4}$$

Equation (4) determines the temperature at the point with coordinates x, y, z by the source position x',y'. In Fig. 1 a temperature distribution in the infinite body caused by instantaneous point source of heat (4) is presented. In calculation the

thermomechanical properties of material are assumed $a = 8 \cdot 10^{-6}$ m^2/s, $c\rho = 5{,}2 \cdot 10^6$ J/m ^{0}C, heat source $Q = 3{,}3 \cdot 10^3$ J and initial temperature $T_0 = 0$.

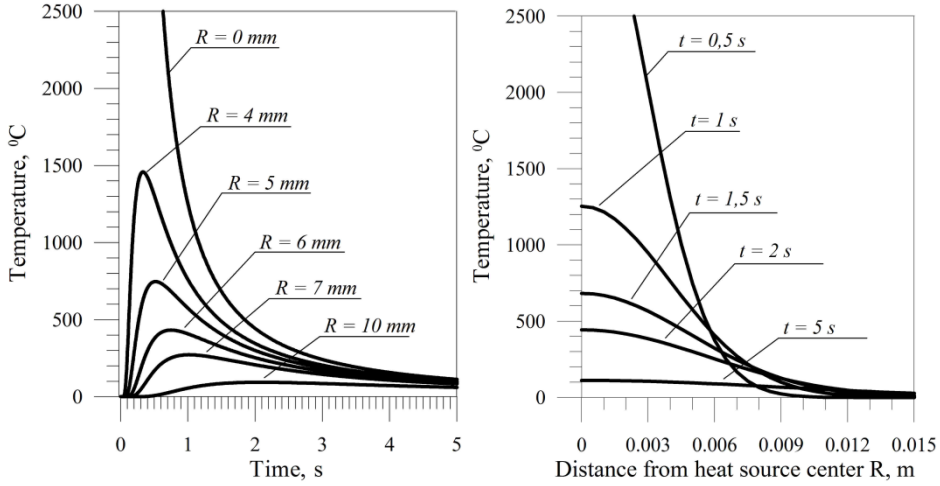

Fig. 1. Temperatures near the temporary heat source: a) heat cycles for points at different distances from the source; b) temperature distribution in the body for some times.

The adoption of a point heat source used in works mentioned above gives for the points located near the center of the weld results significantly deviating from the actual temperature values. Therefore Eagar and Tsai [4] proposed 2D Gaussian distributed heat source model (Fig. 2).

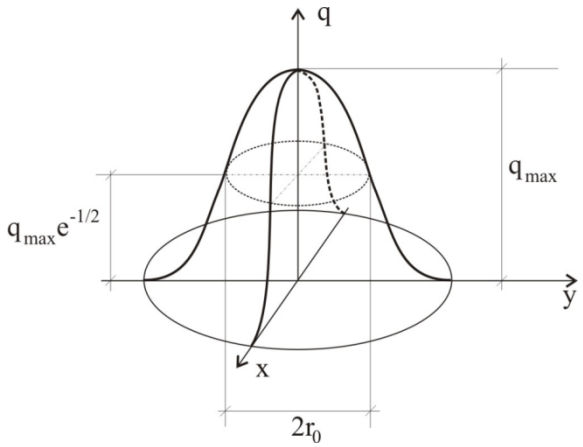

Fig. 2. Two-dimensional Gaussian distributed heat source

Since then many researchers have tried to obtain a solution closest to the real temperature distribution. Double-ellipsoid, three-dimensional heat source (Fig. 3) as the first introduced Goldak [5] (5 - 6).

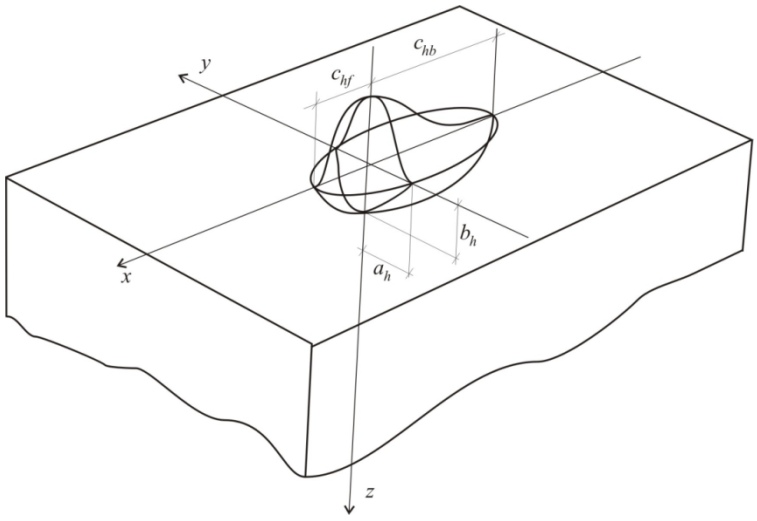

Fig. 5. Double ellipsoidal Goldak's model of heat source

$$Q(x,y,z)=\frac{6\sqrt{3}r_f Q}{a_h b_h c_{hf}\pi\sqrt{\pi}}\exp\left(-\frac{3x^2}{c_{hf}^2}-\frac{3y^2}{a_h^2}-\frac{3z^2}{b_h^2}\right) \tag{5}$$

$$Q(x,y,z)=\frac{6\sqrt{3}r_b Q}{a_h b_h c_{hb}\pi\sqrt{\pi}}\exp\left(-\frac{3x^2}{c_{hb}^2}-\frac{3y^2}{a_h^2}-\frac{3z^2}{b_h^2}\right) \tag{6}$$

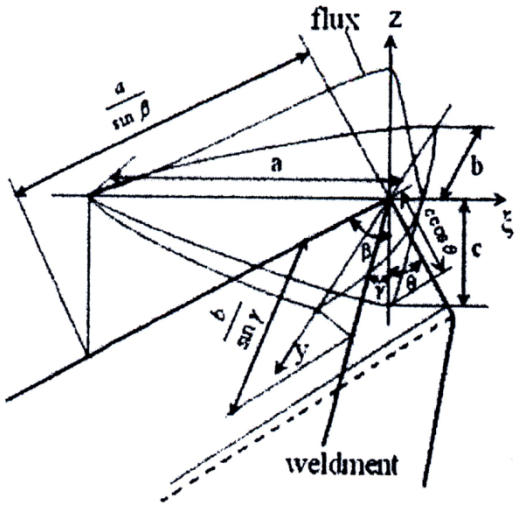

Fig. 6. Double ellipsoidal Goldak's model of heat source

Hongyuan et al. [6] proposed a tilted double ellipsoidal heat source (Fig. 6) (7 – 8) to calculate the temperature field using the finite element method. Importing the energy fraction $f_f + f_r = 2$ gives the heat source formula for forward half ellipsoid:

$$Q(x,y,z,t) = Q(0) f_f \exp\left\{-3[x+v(\tau-t)]^2 / \frac{a^2}{\sin\beta}\right\} \exp\left(-3y^2 / \frac{b^2}{\sin\gamma}\right) \exp\left[-3z^2 / (c\cos\theta)^2\right] \tag{7}$$

and for rear half of ellipsoid:

$$Q(x,y,z,t) = Q(0) f_r \exp\left\{-3[x+v(\tau-t)]^2 / \frac{a^2}{\sin\beta}\right\} \exp\left(-3y^2 / \frac{b^2}{\sin\gamma}\right) \exp\left[-3z^2 / (c\cos\theta)^2\right] \tag{8}$$

In [7] desricption of three dimensional temperature field a volumetric heat source of Gaussian surface distribution is assumed (Fig. 7) with parabolic change in relation to depth (Fig. 8) (9).

$$q_v = q_{\max} \exp\left(-\frac{(x')^2 + (x')^2}{r_B^2}\right)\left(1 - \left(\frac{z'}{z_0}\right)^2\right) \tag{9}$$

where z_0 depth of heat source deposition, and r_B averaging radius of distribution of Gaussian heat source.

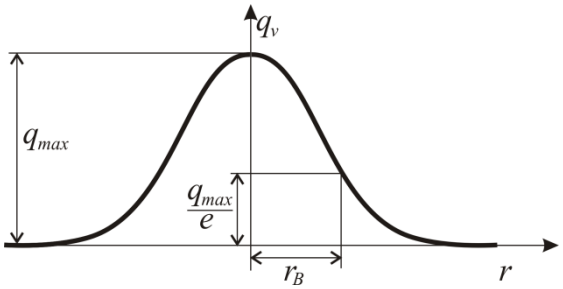

Fig. 7. Gaussian surface distribution of the heat source

Analytical solution of temporary temperature field in half-infinite body caused by moving heat source tilted towards the direction of motion (Fig. 9) is presented in [8] (10 – 12).

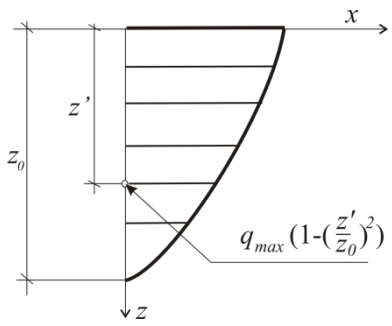

Fig. 8. Parabolic change of the heat source in relation to depth

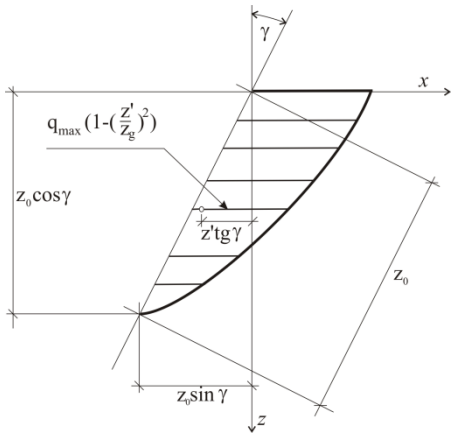

Fig. 9. Distribution of tilted heat source in relation to depth.

$$q_v = q_{\max} \exp\left(-\frac{(x'+z'tg\gamma)^2 + (y')^2}{r_B^2} \right)\left(1-\left(\frac{z'}{z_g} \right)^2 \right) \tag{10}$$

for $z' \in \langle 0, z_g \rangle$ and $-\pi/2 < \gamma < \pi/2$, which fulfills the condition

$$q = \int_{-\infty}^{\infty}\left(\int_{-\infty}^{\infty}\left(\int_{0}^{z_g} q_v dz' \right) dx' \right) dy' \tag{11}$$

where z_g denotes

$$z_g = z_0 \cos\gamma \tag{12}$$

Assumed a single distributed heat source model in the temperature field descriptions does not allow always to reproduce the irregular shapes of the isotherms (including fusion line and heat affected zone limits) occurring in welding

practice. Therefore, in the temperature field modeling of the welding processes the bimodal heat sources are used, especially in hybrid processes (e.g. [9]), but also to surfacing by welding process description [10].

Keywords: **heat source model, temperature filed, welding, modelling**

References

[1] Rosenthal D., Mathematical theory of heat distribution during welding and cutting, Welding J., 20 (1941), 220–234
[2] Rykalin N.N., Tieplovyje osnovy svarki, AN SSSR, Moskva, 1947
[3] Carslaw,H.S., J. C. Jaeger J.C., Conduction of heat in solids, Oxford University Press, 1973.
[4] Eagar T.W., Tsai N.S., Temperature fields produced by traveling distributed heat sources, Welding J., 62 (1983), 346– 355
[5] Goldak J., Chakravarti A., Bibby M., A new finite element model for welding heat sources, Metall. Trans., 15B (1984), 299–305
[6] Hongyuan F., Qingguo M., Wenli X., Shude J., New general double ellipsoid heat source model, Science and Technology Welding and Joining, 2005, 10, 361 –368.
[7] Winczek J., Analytical solution to transient temperature field in a half-infinite body caused by moving volumetric heat source. Int J Heat Mass Transf 53 (2010), 5774-5781
[8] Parkitny R., Winczek J., Analytical solution of temporary temperature field in half-infinite body caused by moving tilted volumetric heat source, Int. J. Heat Mass Transf. 60 (2013), 469 – 479
[9] Piekarska W., Kubiak M., Three-dimensional model for numerical analysis of thermal phenomena in laser-arc hybrid welding process, Int. J. Heat Mass Transfer, 54,2011, 4966-4974
[10] Winczek J., New approach to modeling of temperature field in surfaced steel elements, Int. J. Heat Mass Transf., 54, 2011, 4702–4709.

FINDING THE EXPECTED VOLUMES OF REQUESTS IN QUEUING NETWORK SYSTEMS WITH A LIMITED NUMBER OF EXPECTATIONS

Paweł Zając, Mikhail Matalytski

Institute of Mathematics, Czestochowa University of Technology, Czestochowa, Poland
pawel.zajac@im.pcz.pl, m.matalytski@gmail.com

This presentation describes the method of finding the expected volume of requests in open HM-network without requests the same type of queuing systems. Considered the case when the change in volume associated with transitions between states of the network are deterministic network functions dependent states of network and time, and service systems are single line. It is assumed that the probability of requests network systems, the input stream and requests parameters depend on time.

The work included business model a wireless network, where the network is a collection of wireless access points S_i, each of which gives the user the ability to connect to the network of information by the next available port and use its resources, $i=\overline{1,n}$. Each access point can simultaneously connect multiple users to the network.

An estimate of overall volume of data (data packets) for each wireless access point (WAP) at the given point in time is an important task when designing a wireless network, because it allows to locate the highly loaded WAP and distribute the load evenly over them.

Therefore, you must determine the average total volume of data (packets of users) received by the access points to the network information (eg. Internet), taking into account the limited number of simultaneous connections by this point. This problem can be solved by using HM-network of queuing theory. According to the queuing network (network Q) we mean a set of interconnected systems S_i with a limited buffer size L_i to store the queue of request packet. By network Q understand the user's request to the WAP, which is a data packet.

The analysis of the network without the system around the same type with stream and service parameters. The analysis of the network without the system around the same type of flow parameters and service, time-dependent. Charts volume for such systems may consist of the following form (figures 1-2).

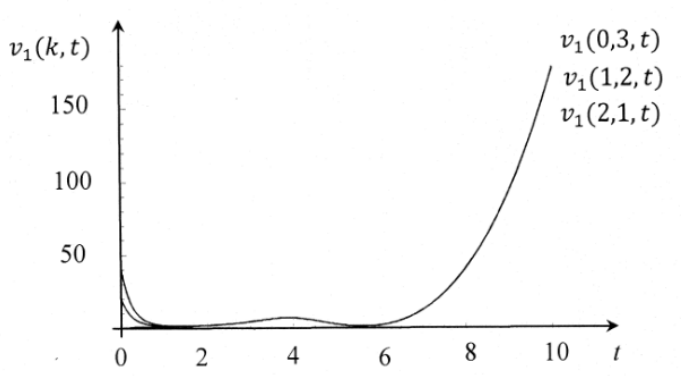

Fig. 1. The volume of requests in the system S_1 for T=[0,10]

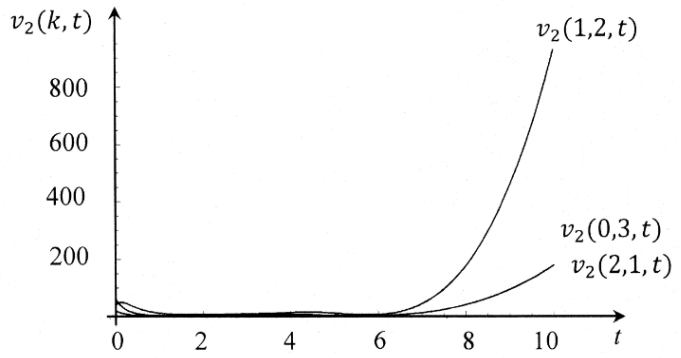

Fig. 2. The volume of requests in the system S_2 for T=[0,10]

Keywords: **queuing networks, volume of requests, HM-networks, wireless access point**

References

[1] Matalytski M.: Analysis and forecasting of expected incomes in Markov networks with servicing systems. Automation and Remote Control, Vol. 76 (11), 2015, s. 2179-2189. (in Russian)
[2] Matalytski M., Kiturko O., Czhornaja N.: Finding expected incomes in HM-Network with priority requests and linear time-dependent intensity of their service. Scientific Research of the Institute of Mathematics and Computer Science of Czestochowa University of Technology, Vol. 10, No. 2, 2011, s. 179-190.
[3] https://pl.wikipedia.org/wiki/IPv4 - data of access: 27.09.2015.

THEORETICAL ASPECTS OF THE APPLICATION OF ARTIFICIAL INTELLIGENCE ALGORITHMS IN THE THERMO-MECHANICAL ISSUES

Maria Zych

Institute of Computer and Information Sciences, Czestochowa University of Technology, Czestochowa, Poland
maria.zych@icis.pcz.pl

The paper shows connection between the selected algorithms and artificial intelligence in the thermo-mechanical issues.

The work presents thermo-mechanical the analysis of the phenomenon illustrated with an example of Fourier equations:

$$\nabla \cdot \left(\lambda \nabla \mathrm{T} \right) = c\rho \frac{\partial \mathrm{T}}{\partial t} \tag{1}$$

where T-the temperature, t- the time , λ-the thermal conductivity, ρ specific heat, c thermal conductivity [1], [2]. The problem of heat conduction belongs to the initially-boundary issues. Initial conditions are used to assign certain values at the initial moment. Four types of boundary conditions that are associated with a complex heat exchange are distinguished [1].

The method involves the use of swarms algorithms in heat conduction. One of the selected algorithms is bee algorithms with allow you to search the solutions to the problem based on the process of acquiring the nectar by bees. Initially, a group of bees scouts in a randomly selected direction distributed aim if the search areas are rich in inflorescence. After returning to the hive, they shall inform other bees about their best discovery. Through bee dance information is transmitted about the quality, direction and distance of food from the hive.

The general scheme of the ABC algorithm is as follows:

Initialization Phase
REPEAT
  Employed Bees Phase
  Onlooker Bees Phase
  Scout Bees Phase
  Memorize the best solution achieved so far
UNTIL(Cycle=Maximum Cycle Number or a Maximum CPU time)

The use of the above methods of artificial intelligence will allow the determination of the parameters used in the equations, numerical initially-boundary issues with boundary conditions of type III and IV.

The third type of boundary condition (Newton): on the boundary Γ of the area Ω the heat exchange with the environment occurs:

$$\Gamma : q = \alpha(\mathrm{T} - \mathrm{T}_{ot}) \tag{2}$$

where α is the coefficient of heat exchange with the environment, T is the temperature of the body on the boundary Γ and *Tot* is the ambient temperature, q is the heat flux entering (T < *Tot*) into the area Ω or the effluent (T> *Tot*) from the area Ω.

The fourth type of boundary condition (continuity condition): on the boundary Γ separating the areas Ω 1 and Ω 2 flow of heat occurs. There are two cases for this boundary condition:

• ideal contact

$$\Gamma : \left\{ \begin{array}{c} (\mathbf{n} \cdot \lambda \nabla T)^{(1)} = (\mathbf{n} \cdot \lambda \nabla T)^{(2)} \\ T^{(1)} = T^{(2)} \end{array} \right\} \tag{3}$$

where ***n*** is the normal vector to the Γ boundary,

• no perfect contact (contact through an additional layer)

$$\Gamma : \left\{ \begin{array}{c} -(\mathbf{n} \cdot \lambda \nabla T)^{(1)} = -(\mathbf{n} \cdot \lambda \nabla T)^{(2)} = \dfrac{\lambda_p}{\delta}\left(T^{(1)} - T^{(2)}\right) \\ T^{(1)} \neq T^{(2)} \end{array} \right\} \tag{4}$$

Keywords: **heat conduction, artificial intelligence algorithms, thermo-mechanical issues**

References

[1] Sczygiol N., Modelowanie numeryczne zjawisk termomechanicznych w krzepnącym odlewie i formie odlewniczej, Wydawnictwo Politechniki Częstochowskiej, Częstochowa 2000.

[2] Sczygiol N., and Szwarc G. Application of enthalpy formulations from numerical simulation of castings solidification. Computer Assisted Mechanics and Engineering Sciences 2011, 8:99-120.

[3] Shen R. Wu, Lumped mass matrix in explicit finite element method for transient dynamics of elasticity, Comput. Methods Appl. Mech. Engrg. 2006, 195, 5983–5994.